

# One-Loop Tachyon Amplitude in Unoriented Open-Closed String Field Theory

Tsuguhiko ASAKAWA,<sup>1,\*</sup> Taichiro KUGO<sup>1,\*\*</sup> and Tomohiko TAKAHASHI<sup>2,\*\*\*</sup>

<sup>1</sup>*Department of Physics, Kyoto University, Kyoto 606-8502*

<sup>2</sup>*Department of Physics, University of Tokyo, Tokyo 113-0033*

(Received June 11, 2021)

We calculate one-loop 2-point tachyon amplitudes in unoriented open-closed string field theory, and determine all the coupling constants of the interaction vertices in the theory. It is shown that the planar, nonplanar and nonorientable amplitudes are all reproduced correctly, and nontrivial consistencies between the determined coupling constants are observed. The necessity for the gauge group to be  $SO(2^{13}=8192)$  is also reconfirmed.

## §1. Introduction

In previous two papers,<sup>1),2)</sup> which we refer to as I and II, we constructed a string field theory (SFT) for an unoriented open-closed string mixed system and proved the BRS/gauge invariance of the action at the ‘tree level’: namely, we have classified the terms in the BRS transform of the action into two categories, ‘tree terms’ and ‘loop terms’ and have shown that all the ‘tree terms’ indeed cancel themselves. And for the other ‘loop terms’, we have identified which anomalous one-loop diagrams they are expected to cancel.

It was left for a future work to show that those loop diagrams are indeed anomalous and the ‘loop terms’ really cancel them. However, the task to show this BRS invariance for general one-loop diagrams is technically rather hard and we have not yet completed it. Here in this paper, we address ourselves to an easier problem to compute the one-loop 2-point (open-string) tachyon amplitudes in our SFT. These one-loop amplitudes already suffer from a BRS anomaly and so the present calculation gives partially an affirmative answer to the above expected cancellation between the ‘loop terms’ and the one-loop anomaly. Moreover with this computation we shall confirm that the one-loop tachyon amplitudes are correctly reproduced in our SFT and can determine all the remaining coupling constants left undetermined in the previous work; in particular, we show that the gauge group must be  $SO(2^{13}=8192)$ .

The action of the present system, containing seven interaction terms, is given by

$$S = -\frac{1}{2} \langle \Psi | \tilde{Q}_B^o \Pi | \Psi \rangle - \frac{1}{2} \langle \Phi | \tilde{Q}_B^e (b_0^- \mathcal{P} \Pi) | \Phi \rangle \\ + \frac{g}{3} \langle V_3^o(1, 2, 3) | | \Psi \rangle_{321} + x_4 \frac{g^2}{4} \langle V_4^o(1, 2, 3, 4) | | \Psi \rangle_{4321} + x_\alpha \frac{g^2}{2} \langle V_\alpha(1, 2) | | \Psi \rangle_{21}$$

---

\* JSPS Research Fellow. E-mail address: asakawa@gauge.scphys.kyoto-u.ac.jp

\*\* E-mail address: kugo@gauge.scphys.kyoto-u.ac.jp

\*\*\* JSPS Research Fellow. E-mail address: tomo@hep-th.phys.s.u-tokyo.ac.jp

$$\begin{aligned}
& +x_c \frac{g^2}{3!} \langle V_3^c(1^c, 2^c, 3^c) | |\Phi\rangle_{321} + x_\infty \frac{g^2}{2} \langle V_\infty(1^c, 2^c) | |\Phi\rangle_{21} \\
& +x_u g \langle U(1, 2^c) | |\Phi\rangle_2 |\Psi\rangle_1 + x_\Omega \frac{g^2}{2} \langle U_\Omega(1, 2, 3^c) | |\Phi\rangle_3 |\Psi\rangle_{21}, \tag{1.1}
\end{aligned}$$

where  $x_4, x_\infty, x_c, x_\Omega, x_u$  and  $x_\Omega$  are coupling constants (relative to the open 3-string coupling constant  $g$ ). For notation and conventions, we follow our previous papers I and II. The open and closed string fields are denoted by  $|\Psi\rangle$  and  $|\Phi\rangle$ , respectively, both of which are Grassmann *odd*. The multiple products of string fields are denoted for brevity as  $|\Psi\rangle_{n\dots 21} \equiv |\Psi\rangle_n \cdots |\Psi\rangle_2 |\Psi\rangle_1$ . The BRS charges  $\tilde{Q}_B$  with tilde here, introduced in I, are given by the usual BRS charges  $Q_B$  plus counterterms for the ‘zero intercept’ proportional to the squared string length parameter  $\alpha^2$ :

$$\tilde{Q}_B^o = Q_B^o + \lambda_o g^2 \alpha^2 c_0, \quad \tilde{Q}_B^c = Q_B^c + \lambda_c g^2 \alpha^2 c_0^+. \tag{1.2}$$

The ghost zero-modes for the closed string are defined by  $c_0^+ \equiv (c_0 + \bar{c}_0)/2$ ,  $c_0^- \equiv c_0 - \bar{c}_0$ , and  $b_0^+ \equiv b_0 + \bar{b}_0$ ,  $b_0^- \equiv (b_0 - \bar{b}_0)/2$ .

The string fields are always accompanied by the unoriented projection operator  $\Pi$ , which is given by using the twist operator  $\Omega$  in the form  $\Pi = (1 + \Omega)/2$ , where  $\Omega$  for the open string case means also taking transposition of the matrix index. The closed string is further accompanied by the projection operator  $\mathcal{P} \equiv \int_0^{2\pi} (d\theta/2\pi) \exp i\theta(L_0 - \bar{L}_0)$ , projecting out the  $L_0 - \bar{L}_0 = 0$  modes, and the corresponding anti-ghost zero-mode factor  $b_0^- = (b_0 - \bar{b}_0)/2$ .

Among the seven vertices, the open 3-string vertex  $V_3^o$ , open-closed transition vertex  $U$  and open-string self-intersection vertex  $V_\infty$  are relevant in this paper and have the following form:<sup>2)</sup>

$$\begin{aligned}
\langle V_3^o(1, 2, 3) | &= \langle v_3^o(1, 2, 3) | \prod_{r=1,2,3} \Pi^{(r)}, \\
\langle U(1, 2^c) | &= \langle u(1, 2^c) | (b_0^- \mathcal{P})^{(2^c)} \prod_{r=1,2^c} \Pi^{(r)}, \\
\langle V_\infty(1, 2) | &= \int_{0 \leq \sigma_1 \leq \sigma_2 \leq \pi \alpha_1} d\sigma_1 d\sigma_2 \langle v_\infty(1, 2; \sigma_1, \sigma_2) | b_{\sigma_1} b_{\sigma_2} \prod_{r=1,2} \Pi^{(r)}. \tag{1.3}
\end{aligned}$$

The vertices here denoted by lower case letters are those constructed by the procedure of LeClair, Peskin and Preitschopf (LPP).<sup>3)</sup> The  $b_{\sigma_r}$  ( $r = 1, 2$ ) are anti-ghost factors<sup>4), 5), 6)</sup> corresponding to the moduli  $\sigma_r$  representing the two interaction points in the intersection vertex  $v_\infty$ . Those LPP vertices generally have the structure

$$\int \left( \prod_r \frac{d^d p_r}{(2\pi)^d} \right) (2\pi)^d \delta^d \left( \sum_r p_r \right) {}_1\langle p_1 | {}_2\langle p_2 | \cdots {}_n\langle p_n | e^{E(\alpha)} \tag{1.4}$$

where  ${}_r\langle p_r |$  is the Fock bra vacuum of string  $r$  with momentum eigenvalue  $p_r$  and the exponent  $E(\alpha)$  is a quadratic form of string oscillators with Neumann coefficients determined by the way of gluing the participating strings. A point to be noted here is that since the gluing way depends on the set of the string lengths  $\alpha_r$  and, in our  $\alpha = p^+$  HIKKO type theory,<sup>7)</sup> the string length  $\alpha_r$  is identified with the +

component of string momentum  $p_r^\mu$ ; i.e.,  $\alpha_r = 2p_r^+$  for open string and  $\alpha_r = p_r^+$  for closed string, the exponent function  $E(\alpha)$  has a nontrivial dependence on  $\alpha_r$ s. Note that  $p^\pm \equiv (p^0 \pm p^{d-1})/\sqrt{2}$  and  $p^2 = -2p^+p^- + \mathbf{p}^2$ . Therefore the integration over  $d^d p = dp^+ dp^- d^{d-2} \mathbf{p}$  in Eq. (1.4) is quite nontrivial.

In the previous papers, we have shown that the theory is BRS (and hence gauge) invariant at ‘tree level’ if the coupling constants satisfy the relations

$$\lambda_c = 2\lambda_o = -\lim_{\epsilon \rightarrow 0} \frac{32nx_u^2}{\epsilon^2}, \quad (1.5)$$

$$x_\infty = nx_u^2 = -4\pi i x_\infty, \quad (1.6)$$

$$x_4 = 1, \quad (1.7)$$

$$x_u = x_\Omega, \quad x_c = 8\pi i x_\Omega, \quad (1.8)$$

where the sign of  $x_\infty$  has been changed from the previous papers I and II since we change the sign convention for the  $V_\infty$  vertex in this paper by the reason as will be made clear in §5. These relations (1.5) – (1.8) leave only two parameters free, e.g.,  $x_u$  and  $n$ , or  $x_u$  and  $x_\infty$ . We shall determine all the three parameters  $x_u$ ,  $x_\infty$  and  $n$ , thus giving a nontrivial consistency check of the theory.

The rest of this paper is organized as follows. First in §2, we show which diagrams contribute to the on-shell tachyon 2-point amplitude at one-loop level by using Feynman rule in the present SFT. To evaluate the amplitudes of those diagrams explicitly we need to conformally map those diagrams into the torus plane and to compute the conformal field theory (CFT) correlation functions on the torus. We present in §3 such conformal mapping for each diagram explicitly, and calculate in §4 the Jacobians for the changes of moduli parameters associated with the mappings. In §5 we first give some discussions on the ‘generalized gluing and resmoothing theorem’ (GGRT)<sup>3), 8)</sup> to fix the normalizations of CFT correlation functions on the torus, and then evaluate the necessary correlation functions explicitly. Gathering those results in §§3 - 5, we finally evaluate the tachyon amplitude explicitly in §6, where the coupling constants  $x_u$  and  $x_\infty$  and  $n$  of the gauge group  $SO(n)$  are also determined. Finally in §7, we conclude and present some discussions on the relations between the BRS anomaly in the present SFT and the Lorentz invariance anomaly in the light-cone gauge SFT.<sup>9), 10), 11)</sup>

For the variables and functions appearing in the one-loop amplitudes, we use the same notations as much as possible as those in Chapter 8 of the textbook by Green, Schwarz and Witten (GSW).<sup>12)</sup> We cite in Appendix some modular transformation relations between such one-loop functions which will be used in the text.

## §2. One-loop 2-point tachyon amplitude: preliminaries

The one-loop amplitude obtained by using open 3-string vertex  $V_3^o$  twice contributes to the effective action  $\Gamma_{1\text{-loop}}$  at one loop as

$$\Gamma_{1\text{-loop}} = i^{-1} \frac{1}{2!} 2 \cdot 3 \cdot 3 \left( \frac{g}{3} \right)^2 \langle V_3^o(C, E, 1) | \Psi \rangle_1 \overbrace{\langle \Psi \rangle_E | \Psi \rangle_C \langle V_3^o(D, 2, F) | \Psi \rangle_F | \Psi \rangle_2 | \Psi \rangle_D}$$

$$\begin{aligned}
&= -ig^2 \langle V_3^o(C, E, 1) | \langle V_3^o(D, 2, F) | \overline{|\Psi\rangle_C |\Psi\rangle_D} \overline{|\Psi\rangle_E |\Psi\rangle_F} |\Psi\rangle_2 |\Psi\rangle_1 \\
&= ig^2 \int_0^\infty d\tau_1 d\tau_2 \langle \tilde{V}(1, 2; \tau_1, \tau_2) | b_{\tau_1} b_{\tau_2} |\Psi\rangle_2 |\Psi\rangle_1,
\end{aligned} \tag{2.1}$$

where\* the open string propagator is given by

$$\begin{aligned}
\overline{|\Psi\rangle_C |\Psi\rangle_D} &\equiv \left( \frac{b_0}{L_0} \right)^{(C)} |R^o(C, D)\rangle = \left( \frac{b_0}{L_0} \right)^{(D)} |R^o(C, D)\rangle \\
&= \int_0^\infty dT_1 b_0^{(D)} e^{-L_0^{(D)} T_1} |R^o(C, D)\rangle = \int_0^\infty d\tau_1 b_{\tau_1} e^{-L_0 \tau_1} |R^o(C, D)\rangle
\end{aligned} \tag{2.2}$$

and the glued vertex  $\langle \tilde{V}(1, 2; \tau_1, \tau_2) |$  is defined by

$$\langle \tilde{V}(1, 2; \tau_1, \tau_2) | \equiv \langle V_3^o(C, E, 1) | \langle V_3^o(D, 2, F) | e^{-L_0 \tau_1} |R^o(C, D)\rangle e^{-L_0 \tau_2} |R^o(E, F)\rangle. \tag{2.3}$$

Here  $\tau_1 = \alpha_D T_1$  is the time interval on the  $\rho$  plane defined later and  $b_{\tau_1} = \alpha_D^{-1} b_0^{(D)}$  is the anti-ghost factor corresponding to the moduli  $\tau_1$ . Our SFT vertex  $\langle V_3^o(1, 2, 3) |$  contains the unoriented projection operators  $\Pi^{(i)} = (1 + \Omega^{(i)})/2$  ( $i = 1, 2, 3$ ), as an effect of which the propagators of the two intermediate strings  $D$  and  $F$  are multiplied by the projection operators:

$$\begin{aligned}
\langle \tilde{V}(1, 2; \tau_1, \tau_2) | &= \langle v_3^o(C, E, 1) | \langle v_3^o(D, 2, F) | \\
&\times \Pi^{(D)} \Pi^{(F)} e^{-L_0 \tau_1} |R^o(C, D)\rangle e^{-L_0 \tau_2} |R^o(E, F)\rangle \prod_{r=1}^2 \Pi^{(r)}.
\end{aligned} \tag{2.4}$$

This product of projection operators yields four terms,  $\Pi^{(D)} \Pi^{(F)} = (1 + \Omega^{(D)} + \Omega^{(F)} + \Omega^{(D)} \Omega^{(F)})/4$ , and accordingly the glued vertex  $\langle \tilde{V}(1, 2; \tau_1, \tau_2) |$  contains four different configurations as drawn in Fig. 1, which we call planar (P), nonorientable (or Möbius) (M1 and M2) and nonplanar (NP) diagrams, respectively. To those the following four LPP vertices correspond:

$$\langle \tilde{V}(1, 2; \tau_1, \tau_2) | = \frac{1}{4} \left\{ n \langle v_P(\tau_1, \tau_2) | + \langle v_{M1}(\tau_1, \tau_2) | + \langle v_{M2}(\tau_1, \tau_2) | + \langle v_{NP}(\tau_1, \tau_2) | \right\} \prod_{r=1}^2 \Pi^{(r)} \tag{2.5}$$

where the factor  $n$  in front of  $\langle v_P |$  has come from the inner endpoint loop carrying Chan-Paton index in the planar diagram.

We take the external open string states to be on-shell tachyon states

$$|\Psi\rangle_r = |\varphi^0(k_r)\rangle_r = \left[ c(w_r) e^{ik_r \cdot X^{(r)}(w_r)} \right]_{w_r=0} |0\rangle_r \quad (k_r^2 = 2). \tag{2.6}$$

Then, the one-loop effective action (2.1) with Eq. (2.5) substituted, yields the following one-loop 2-point tachyon amplitudes

$$\{ \mathcal{A}_P + \mathcal{A}_{M1} + \mathcal{A}_{M2} + \mathcal{A}_{NP} \} \delta_{k_1 + k_2}$$

---

\* Note that the factor  $i^{-L}$  is multiplied to the  $L$ -loop level effective action in the present Feynman rule where the factors  $i^{-1}$  and  $i$  are omitted from the propagators and the vertices, respectively.

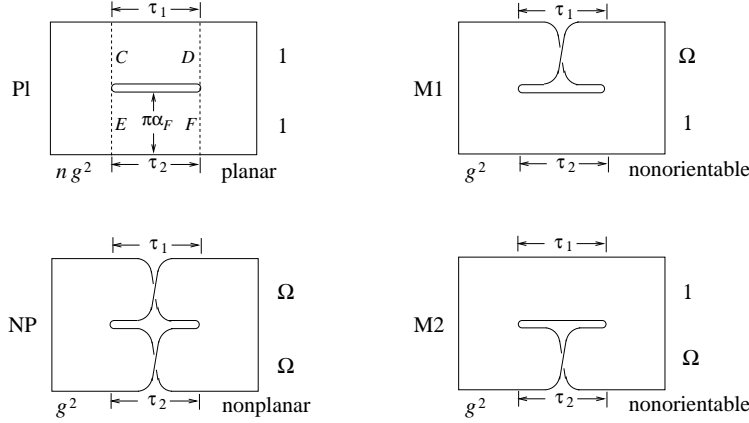


Fig. 1. Four diagrams contributing to the one-loop 2-point amplitude. For tachyon external states, actually, only the configurations with  $\tau_1 = \tau_2$  contribute as we shall see later.

$$= 2i \cdot \frac{g^2}{4} \int_0^\infty d\tau_1 d\tau_2 \left\{ n \langle v_P(\tau_1, \tau_2) | + \langle v_{M1}(\tau_1, \tau_2) | + \langle v_{M2}(\tau_1, \tau_2) | \right. \\ \left. + \langle v_{NP}(\tau_1, \tau_2) | \right\} b_{\tau_1} b_{\tau_2} |\varphi^0(k_2)\rangle_2 |\varphi^0(k_1)\rangle_1, \quad (2.7)$$

with an abbreviation  $\delta_{k_1+k_2} \equiv (2\pi)^d \delta^d(k_1 + k_2)$ , where the individual amplitude is evaluated by the CFT on the corresponding torus  $J = P, M1, M2, NP$ :

$$\langle v_J(\tau_1, \tau_2) | b_{\tau_1} b_{\tau_2} |\varphi^0(k_2)\rangle_2 |\varphi^0(k_1)\rangle_1 = \left\langle b_{\tau_1} b_{\tau_2} c(Z_2) e^{ik_2 \cdot X(Z_2)} c(Z_1) e^{ik_1 \cdot X(Z_1)} \right\rangle_J. \quad (2.8)$$

Here we note two points. First, the RHS is generally multiplied by a factor

$$\prod_{r=1,2} \left( \frac{du}{dw_r} \right)_{u=Z_r}^{\frac{k_r^2}{2}-1} \quad (2.9)$$

which is associated with the conformal mapping of the operators  $c(w_r) e^{ik_r \cdot X(w_r)}$  from the unit disk  $w_r$  to the torus  $u$  plane and  $Z_r = u(w_r=0)$  are the positions of punctures on the torus representing the external strings. But here the factor (2.9) is 1 since the conformal weights  $(k_r^2/2) - 1$  are zero for the *on-shell* tachyons. Secondly, this Eq. (2.8) *determines* the CFT correlation functions on the RHS including their signs and weights. This constitutes the content of GGRT;<sup>8), 13)</sup> namely, the loop level LPP vertex  $\langle v_J |$  with  $J = P, NO$  (M1 and M2), NP are already *defined* above as glued vertices of the two tree level LPP vertices  $\langle v_3^0 |$  by Eq. (2.4) with (2.5). So these torus correlation functions are already fixed including their coefficients. We defer the explicit evaluation of these correlation functions until §5.

Here we first consider the nonplanar diagram NP, for which the two intermediate strings are both twisted. The amplitude  $\mathcal{A}_{NP}$  corresponding to this diagram alone does not give the full nonplanar amplitude correctly. Indeed, this can easily be seen if we redraw the diagram NP in the form as depicted in the diagram (a) in Fig. 2. So it can cover only the  $\tau_1 > 0$  part of the full nonplanar amplitude, and the remaining

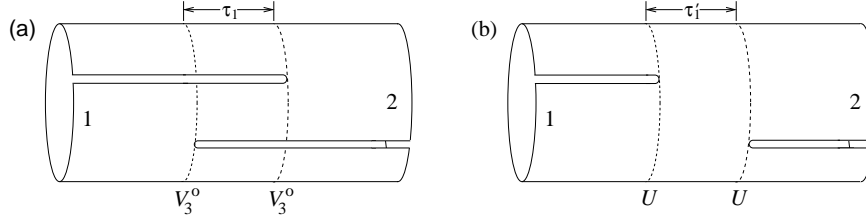


Fig. 2. (a) Loop diagram equivalent to the nonplanar diagram NP in Fig. 1. (b) A tree nonplanar diagram obtained by using the  $U$  vertex twice.

$0 > \tau_1 (= -\tau_1')$  part is supplied by the ‘tree’ diagram given by using the open-closed transition vertex  $U$  twice as drawn in the diagram (b) in Fig. 2.<sup>14)</sup> The amplitude for this  $UU$  diagram is given by

$$\begin{aligned} \mathcal{A}_{UU} \delta_{k_1+k_2} &= \frac{1}{2!} \cdot 2 (x_u g)^2 \langle U(1, A^c) | \overline{|\Phi\rangle_{A^c} |\varphi^0(k_1)\rangle_1} \langle U(2, B^c) | \overline{|\Phi\rangle_{B^c} |\varphi^0(k_2)\rangle_2} \\ &= x_u^2 g^2 \int d\tau_1 \frac{d\sigma_1}{2\pi} \langle v_{UU}(\tau_1, \sigma_1) | b_0 \bar{b}_0 |\varphi^0(k_2)\rangle_2 |\varphi^0(k_1)\rangle_1, \end{aligned} \quad (2.10)$$

where the Wick contraction gives the closed string propagator

$$\begin{aligned} (b_0^- \mathcal{P})^{(A^c)} | \overline{|\Phi\rangle_{A^c} (b_0^- \mathcal{P})^{(B^c)} |\Phi\rangle_{B^c}} &= \left( \frac{b_0 \bar{b}_0}{L_0 + \bar{L}_0} \right)^{(B^c)} \mathcal{P}^{(B^c)} | R^c(A^c, B^c) \rangle \\ &= \int d\tau_1 \frac{d\sigma_1}{2\pi} e^{-(L_0 + \bar{L}_0)\tau_1} e^{-i\sigma_1(L_0 - \bar{L}_0)} b_0 \bar{b}_0 | R^c(A^c, B^c) \rangle \end{aligned} \quad (2.11)$$

and the following glued LPP vertex has been defined:

$$\langle v_{UU}(\tau_1, \sigma_1) | = \langle u(1, A^c) | \langle u(2, B^c) | e^{-(L_0 + \bar{L}_0)\tau_1} e^{-i\sigma_1(L_0 - \bar{L}_0)} | R^c(A^c, B^c) \rangle. \quad (2.12)$$

Again the amplitude is evaluated by referring to the CFT on the torus:

$$\langle v_{UU}(\tau_1, \sigma_1) | b_0 \bar{b}_0 |\varphi^0(k_2)\rangle_2 |\varphi^0(k_1)\rangle_1 = \left\langle b_0 \bar{b}_0 c(Z_2) e^{ik_2 \cdot X(Z_2)} c(Z_1) e^{ik_1 \cdot X(Z_1)} \right\rangle_{UU}. \quad (2.13)$$

The amplitudes  $\mathcal{A}_{NP}$  in Eq. (2.7) and  $\mathcal{A}_{UU}$  in Eq. (2.10) should smoothly connect with each other at  $\tau_1 = 0$  to reproduce the correct nonplanar amplitude, and this condition will determine the coupling constant  $x_u$ , as we shall obtain later.

Next consider the two nonorientable diagrams, M1 and M2 terms in Fig. 1. These two diagrams alone do not give the full nonorientable amplitude, again. Indeed, the two diagrams do not connect with each other at the moduli  $\tau_1 = 0$ , so that another diagram should exist which interconnects these two configurations at  $\tau_1 = 0$ . Such a diagram is just given by the ‘tree’ diagram drawn in Fig. 3 which is obtained by using the  $V_\infty$  vertex. Clearly the configuration of this diagram coincides at  $\sigma_2 = \pi\alpha_1$  (and  $\sigma_1 = \pi\alpha_F$ ) with that of the M1 diagram at  $\tau_1 = 0$ , and at  $\sigma_1 = 0$  (and  $\sigma_2 = \pi\alpha_F$ ) with that of the M2 diagram at  $\tau_1 = 0$ . The amplitude  $\mathcal{A}_{V_\infty}$  of this diagram is proportional to  $x_\infty$ , and so the smooth connection condition for these amplitudes

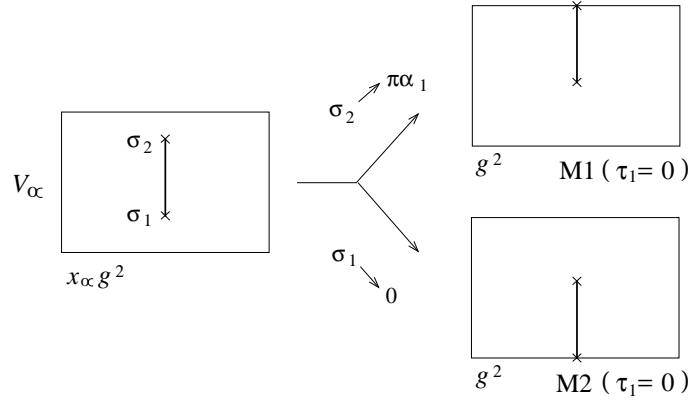


Fig. 3. Tree diagram given by  $V_\infty$  vertex which fill in the gap between the two configurations at  $\tau_1 = 0$  of the nonorientable diagrams M1 and M2 in Fig. 1.

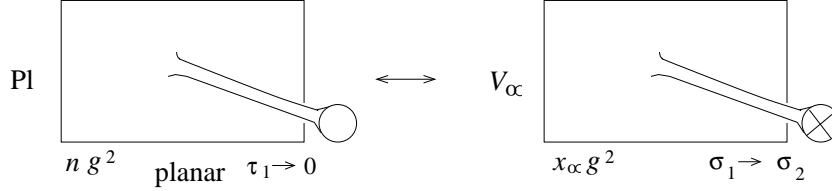


Fig. 4. Singular configurations for the planar diagram and  $V_\infty$  diagram.

will determine  $x_\alpha$  as we shall see later. The amplitude  $\mathcal{A}_{V_\infty}$  is given by

$$\begin{aligned}
 \mathcal{A}_{V_\infty} \delta_{k_1+k_2} &= 2 \cdot x_\alpha \frac{g^2}{2} \langle V_\infty(1,2) | \varphi^0(k_2) \rangle_2 | \varphi^0(k_1) \rangle_1 \\
 &= x_\alpha g^2 \int d\sigma_1 d\sigma_2 \langle v_\infty(1,2; \sigma_1, \sigma_2) | b_{\sigma_1} b_{\sigma_2} | \varphi^0(k_2) \rangle_2 | \varphi^0(k_1) \rangle_1 \\
 &= x_\alpha g^2 \int d\sigma_1 d\sigma_2 \left\langle b_{\sigma_1} b_{\sigma_2} c(Z_2) e^{ik_2 \cdot X(Z_2)} c(Z_1) e^{ik_1 \cdot X(Z_1)} \right\rangle_{V_\infty}. \quad (2.14)
 \end{aligned}$$

Finally, we note that the planar diagram in Fig. 1 as  $\tau_1 \rightarrow 0$  and the above diagram of  $V_\infty$  vertex as  $\sigma_1 - \sigma_2 \rightarrow 0$ , both have singularities owing to the closed tachyon and dilaton vanishing into vacuum. As is shown in Fig. 4, this is almost the same situation as what we have encountered in the disk and  $RP^2$  amplitudes for closed tachyon 2-point function in the previous paper I. The former planar amplitude is proportional to  $ng^2$  and the latter  $V_\infty$  amplitude to  $x_\alpha$ . The condition for the dilaton contributions to cancel between the two amplitudes will determine  $n$  of  $SO(n)$ , as we shall explicitly see later.

### §3. Conformal mapping of $\rho$ plane to torus

In order to calculate these amplitudes in Eqs. (2.7), (2.10) and (2.14), we need conformal mapping of the usual unit disk  $|w_r| \leq 1$  of participating string  $r$  to the torus for each case. The string world sheets of the ‘light-cone type’ diagrams like

Figs. 1, 2 etc, are called  $\rho$  plane, on which the complex coordinate  $\rho = \tau + i\sigma$  is identified with  $\rho = \alpha_r \rho_r + i\beta_r$  ( $\beta_r$ : a real constant) in each string  $r$  strip ( $\text{Re} \rho_r \leq 0$ ), where  $\rho_r = \tau_r + i\sigma_r$  is the image of the unit disk  $|w_r| \leq 1$  of string  $r$  by a simple (conformal) mapping  $\rho_r = \ln w_r$ . Therefore we have only to know the conformal mapping of the  $\rho$  plane to the torus for each case.

The conformal mapping of the  $\rho$  plane to the torus  $u$  plane with periods 1 and  $\tau$  is generically given by the following (generalized) Mandelstam mapping:<sup>15), 12), 16)</sup>

$$\rho(u) = \sum_{r=1,2} \alpha_r \ln \vartheta_1(u - Z_r | \tau) + Au \quad (3.1)$$

where  $\vartheta_i(\nu | \tau)$  ( $i = 1, \dots, 4$ ) are Jacobi  $\vartheta$  functions with periods 1 and  $\tau$ . This  $\rho$  satisfies a quasi-periodicity

$$\rho(u + m\tau + n) - \rho(u) = 2\pi i m \sum_{r=1,2} \alpha_r Z_r + A(m\tau + n). \quad (3.2)$$

The derivative  $d\rho/du$  is truly a doubly periodic function, or *elliptic function*,<sup>17)</sup> which is analytic except for the poles at  $u = Z_r$  ( $r = 1, 2$ ):

$$\frac{d\rho}{du} = \sum_{r=1,2} \alpha_r g_1(u - Z_r | \tau) + A, \quad (3.3)$$

where  $g_i$  is the logarithmic derivative of the Jacobi  $\vartheta$  function:

$$g_i(\nu | \tau) \equiv \frac{\vartheta'_i(\nu | \tau)}{\vartheta_i(\nu | \tau)}, \quad \vartheta'_i(\nu | \tau) \equiv \frac{\partial \vartheta_i(\nu | \tau)}{\partial \nu}. \quad (3.4)$$

$Z_r$  corresponds to the image of the external string  $r$  at  $\tau_r = -\infty$  ( $w_r = 0$ ). Two interaction points  $z_0^{(i)}$  ( $i = 1, 2$ ) are given by the zeros of this function:

$$\frac{d\rho}{du}(z_0^{(i)}) = 0 \quad \Rightarrow \quad \sum_{r=1,2} \alpha_r g_1(z_0^{(i)} - Z_r | \tau) + A = 0. \quad (3.5)$$

By a general property of elliptic functions,<sup>17)</sup> a sum rule holds:

$$Z_1 + Z_2 = z_0^{(1)} + z_0^{(2)} \pmod{\text{periods 1 and } \tau} \quad (3.6)$$

We now examine the conformal mappings for the cases of planar, nonorientable, nonplanar,  $V_\infty$  and  $UU$  diagrams, separately, and will find relations which determine the torus moduli  $\tau$ , the parameter  $A$  and interaction points  $z_0^{(i)}$  in terms of the string length and the moduli parameters of the  $\rho$  plane.

### 3.1. Planar diagram ( $P$ )

The mapping for the planar diagram case is drawn in Fig. 5. In this case the period  $\tau$  is purely imaginary and denoted by  $\tilde{\tau}$ , and the mapping of this Fig. 5 is given by the above Mandelstam mapping (3.1) with  $\tau$  replaced by  $\tilde{\tau}$ . The interaction points  $\rho_0^{(i)}$  in the  $\rho$  plane are mapped to  $z_0^{(i)}$  in the  $u$  plane. By using the shift invariance on



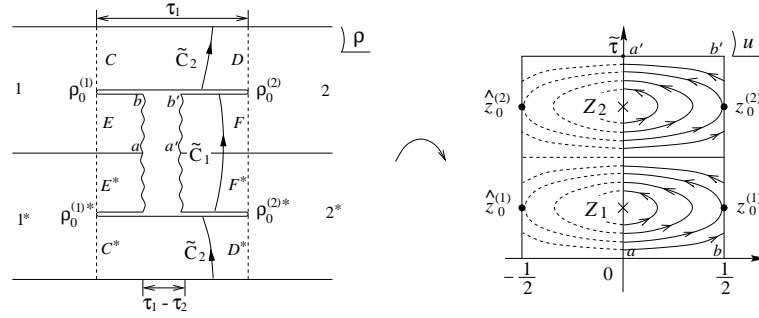


Fig. 5. Conformal mapping of planar diagram  $\rho$  plane to a torus  $u$  plane. In the  $\rho$  plane, the edge curve  $a$ - $b$  of string  $E$  is identified with the curve  $a'$ - $b'$  of string  $F$ , which are mapped to the bottom and top lines  $a$ - $b$  and  $a'$ - $b'$  on the  $u$  plane, respectively.

the torus plane and the sum rule (3.6), we can parametrize the positions of strings (punctures) and interaction points by two real parameters  $x$  and  $y$  as

$$\begin{cases} Z_1 = \tilde{\tau} \left( \frac{1}{2} - x \right) \\ Z_2 = \tilde{\tau} \left( \frac{1}{2} + x \right) \end{cases}, \quad \begin{cases} z_0^{(1)} = \frac{1}{2} + \tilde{\tau} \left( \frac{1}{2} - y \right) \\ z_0^{(2)} = \frac{1}{2} + \tilde{\tau} \left( \frac{1}{2} + y \right) \end{cases}. \quad (3.7)$$

By the help of the periodicity (3.2), we can determine the parameters  $A$  and  $x$  as follows. First, taking  $u + 1 = z_0^{(i)}$ , for instance, we have  $u = \hat{z}_0^{(i)}$  and then  $\rho(u + 1) = \rho_0^{(i)}$  and  $\rho(u) = \rho_0^{(i)*}$ , so that

$$\rho(u + 1) - \rho(u) = A = \rho_0^{(i)} - \rho_0^{(i)*} = 2\pi i \alpha_F \quad \Rightarrow \quad A = 2\pi i \alpha_F. \quad (3.8)$$

Next, note that the bottom line  $\text{Im}u = 0$  and the top line  $\text{Im}u = |\tilde{\tau}|$  with  $0 \leq \text{Re}u \leq 1/2$ , are mapped to the wavy curves  $a$ - $b$  and  $a'$ - $b'$  of strings  $E$  and  $F$  on the  $\rho$  plane in Fig. 5. Therefore we have

$$\begin{aligned} \tau_1 - \tau_2 &= \rho(u + \tilde{\tau}) - \rho(u) = 2\pi i \alpha_1 (Z_1 - Z_2) + A \tilde{\tau} \\ \Rightarrow \quad \frac{\tau_1}{\alpha_1} - \frac{\tau_2}{\alpha_1} &= 2\pi i \tilde{\tau} \left( \frac{\alpha_F}{\alpha_1} - 2x \right). \end{aligned} \quad (3.9)$$

The time length  $\tau_1$  of the intermediate C-D propagator can be connected to the torus parameter  $\tilde{\tau}$  as follows:

$$\begin{aligned} \tau_1 &= \rho_0^{(2)} - \rho_0^{(1)} = \rho(z_0^{(2)}) - \rho(z_0^{(1)}) = 2\alpha_1 \ln \frac{\vartheta_1(z_0^{(1)} - Z_2|\tilde{\tau})}{\vartheta_1(z_0^{(1)} - Z_1|\tilde{\tau})} + A(z_0^{(2)} - z_0^{(1)}) \\ \Rightarrow \quad \frac{\tau_1}{\alpha_1} &= 2 \ln \frac{\vartheta_2(\tilde{\tau}(x + y)|\tilde{\tau})}{\vartheta_2(\tilde{\tau}(x - y)|\tilde{\tau})} + 4\pi i \frac{\alpha_F}{\alpha_1} \tilde{\tau} y. \end{aligned} \quad (3.10)$$

The Eq. (3.5) determining the interaction points, or  $y$ , now reads

$$g_2(\tilde{\tau}(x + y)|\tilde{\tau}) + g_2(\tilde{\tau}(x - y)|\tilde{\tau}) = -2\pi i \frac{\alpha_F}{\alpha_1}, \quad (3.11)$$

which is identical with the extremum condition  $\partial\tau_1/\partial y = 0$  of  $\tau_1$  in Eq. (3.10).

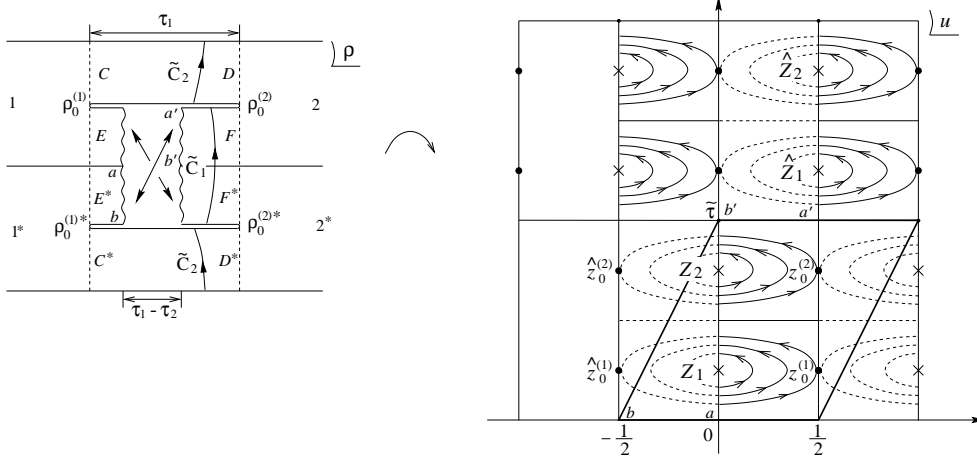


Fig. 6. Conformal mapping of the  $\rho$  plane of nonorientable diagram M1 to a torus. In the  $\rho$  plane, the curve  $a$ - $b$  is identified with the curve  $a'$ - $b'$ , whose images in the  $u$  plane are also shown.

### 3.2. Nonorientable diagrams (M1 and M2)

The mapping of the nonorientable diagram M1 to torus is drawn in Fig. 6. In this case the fundamental region of the torus is given as indicated in the same figure Fig. 6, and so the period  $\tau$  is now given by  $\tilde{\tau} + 1/2$ . Accordingly, the mapping of this Fig. 6 is given by the above Mandelstam mapping (3.1) with  $\tau = \tilde{\tau} + 1/2$ . We can parametrize the positions of strings (punctures) and interaction points by the same equations as Eq. (3.7) in this case also.

Similarly to the previous planar case, the periodicity (3.2) determines the parameters  $A$  and  $x$ ; from the period 1 we have the same relation as before,

$$A = 2\pi i \alpha_F. \quad (3.12)$$

Noting that two points separated by  $\tilde{\tau} + 1/2$ , e.g., the points  $a$  and  $a'$ , on the  $u$  plane correspond to those separated by  $\tau_1 - \tau_2 + i\pi\alpha_F$  on the  $\rho$  plane as seen in Fig. 6, and using the period  $\tilde{\tau} + \frac{1}{2}$  of  $\rho(u)$ , we obtain

$$\begin{aligned} \tau_1 - \tau_2 + i\pi\alpha_F &= \rho(u + (\tilde{\tau} + \frac{1}{2})) - \rho(u) = 2\pi i \alpha_1 (Z_1 - Z_2) + A(\tilde{\tau} + \frac{1}{2}) \\ \Rightarrow \frac{\tau_1}{\alpha_1} - \frac{\tau_2}{\alpha_1} &= 2\pi i \tilde{\tau} \left( \frac{\alpha_F}{\alpha_1} - 2x \right). \end{aligned} \quad (3.13)$$

Equations for  $\tau_1$  and the interaction point  $y$  take the same form as those for the previous planar case aside from the period:

$$\frac{\tau_1}{\alpha_1} = 2 \ln \frac{\vartheta_2(\tilde{\tau}(x+y)|\tilde{\tau} + \frac{1}{2})}{\vartheta_2(\tilde{\tau}(x-y)|\tilde{\tau} + \frac{1}{2})} + 4\pi i \frac{\alpha_F}{\alpha_1} \tilde{\tau} y, \quad (3.14)$$

$$g_2(\tilde{\tau}(x+y)|\tilde{\tau} + \frac{1}{2}) + g_2(\tilde{\tau}(x-y)|\tilde{\tau} + \frac{1}{2}) = -2\pi i \frac{\alpha_F}{\alpha_1}. \quad (3.15)$$

### 3.3. Nonplanar diagram (NP)

The mapping of the nonplanar diagram NP to torus is drawn in Fig. 7. The

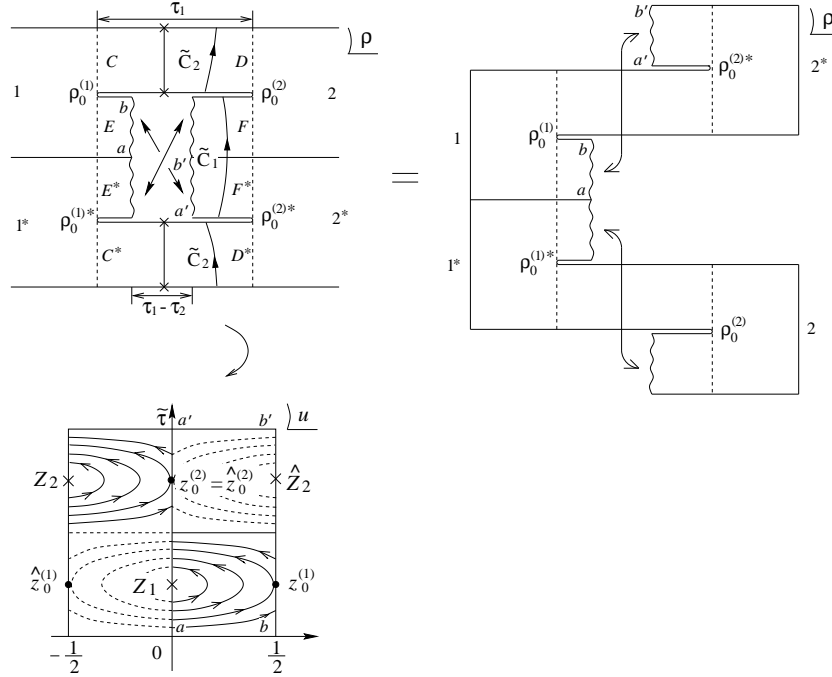


Fig. 7. Conformal mapping of the  $\rho$  plane of nonplanar diagram NP to a torus. In the  $\rho$  plane, the line connecting two crosses denotes twisting, and the curve  $a-b$  is identified with the curve  $a'-b'$ , whose images in the  $u$  plane are also shown.

period  $\tau$  in this case is  $\tilde{\tau}$ , the same as in planar case, and so is the Mandelstam mapping (3.1) with  $\tau = \tilde{\tau}$ . However, the strings (punctures) and interaction points are placed differently from the planar case as shown in Fig. 7. So we parametrize their positions by real parameters  $x$  and  $y$  as

$$\begin{cases} Z_1 = \tilde{\tau} \left( \frac{1}{2} - x \right) \\ Z_2 = -\frac{1}{2} + \tilde{\tau} \left( \frac{1}{2} + x \right) \end{cases}, \quad \begin{cases} z_0^{(1)} = \frac{1}{2} + \tilde{\tau} \left( \frac{1}{2} - y \right) \\ z_0^{(2)} = \tilde{\tau} \left( \frac{1}{2} + y \right) \end{cases}. \quad (3.16)$$

From the period 1 and  $\rho_0^{(1)} - \rho_0^{(1)*} = 2\pi i \alpha_F$ , we again obtain the same relation as before,

$$A = 2\pi i \alpha_F. \quad (3.17)$$

Noting that two points separated by  $\tilde{\tau}$ , e.g., the points  $a$  and  $a'$ , on the  $u$  plane correspond to those separated by  $\tau_1 - \tau_2 + \pi i \alpha_1$  on the  $\rho$  plane as seen in Fig. 7, and using the period  $\tilde{\tau}$  of  $\rho(u)$ , we find

$$\begin{aligned} \tau_1 - \tau_2 + \pi i \alpha_1 &= \rho(u + \tilde{\tau}) - \rho(u) = 2\pi i \alpha_1 (Z_1 - Z_2) + A \tilde{\tau} \\ \Rightarrow \frac{\tau_1}{\alpha_1} - \frac{\tau_2}{\alpha_1} &= 2\pi i \tilde{\tau} \left( \frac{\alpha_F}{\alpha_1} - 2x \right). \end{aligned} \quad (3.18)$$

Equations for  $\tau_1$  and the interaction point  $y$  become in this case

$$\tau_1 + \pi i (\alpha_1 - \alpha_F) = \rho_0^{(2)*} - \rho_0^{(1)} = \rho(\hat{z}_0^{(2)}) - \rho(z_0^{(1)})$$

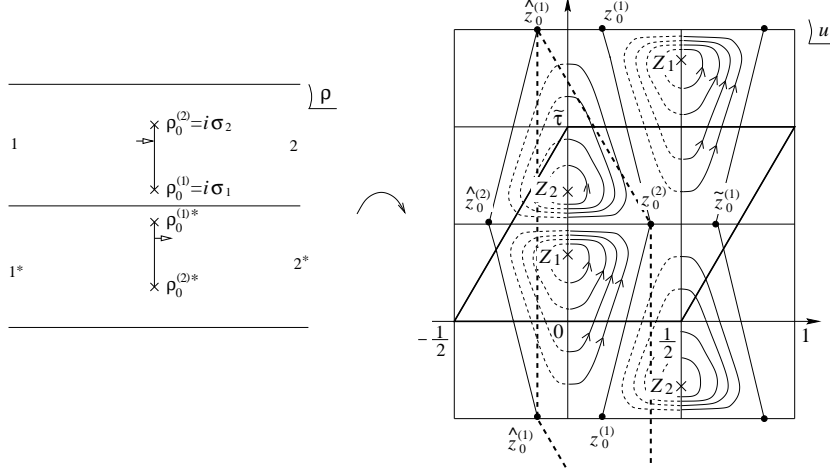


Fig. 8. Conformal mapping of the  $\rho$  plane of  $V_\infty$  diagram to a torus. In the  $\rho$  plane, the lines connecting two crosses denote crosscaps across which the left edge in the upper plane is identified with the right edge in the lower plane. In the  $u$  plane, the parallelogram enclosed by bold solid line denotes a fundamental region of the torus corresponding to the moduli  $\tilde{\tau} + 1/2$ , while that enclosed by bold dotted line denotes another choice of fundamental region corresponding to the moduli  $\tau/4 + 1/2$  used later.

$$\begin{aligned}
 &= 2\alpha_1 \ln \frac{\vartheta_1(z_0^{(1)} - Z_2|\tilde{\tau})}{\vartheta_1(z_0^{(1)} - Z_1|\tilde{\tau})} + A(z_0^{(2)} - z_0^{(1)}) \\
 \Rightarrow \quad \frac{\tau_1}{\alpha_1} &= 2 \ln \frac{\vartheta_1(\tilde{\tau}(x+y)|\tilde{\tau})}{\vartheta_2(\tilde{\tau}(x-y)|\tilde{\tau})} + 4\pi i \frac{\alpha_F}{\alpha_1} \tilde{\tau} y - \pi i, \quad (3.19)
 \end{aligned}$$

$$g_1(\tilde{\tau}(x+y)|\tilde{\tau}) + g_2(\tilde{\tau}(x-y)|\tilde{\tau}) = -2\pi i \frac{\alpha_F}{\alpha_1}. \quad (3.20)$$

### 3.4. $V_\infty$ diagram

The diagram obtained by using  $V_\infty$  vertex once is a tree diagram from the SFT viewpoint, but is actually a one-loop diagram from the CFT point of view. The mapping of the  $V_\infty$  diagram to torus is drawn in Fig. 8. The period  $\tau$  in this case is  $\tilde{\tau} + 1/2$ , as is seen from the fundamental region of the torus in Fig. 8. The two interaction points in the fundamental region are

$$\begin{cases} \tilde{z}_0^{(1)} = z_0^{(1)} + (\tilde{\tau} + \frac{1}{2}) = \hat{z}_0^{(2)} + 1, \\ z_0^{(2)} = \hat{z}_0^{(1)} + (\tilde{\tau} + \frac{1}{2}) \end{cases}, \quad (3.21)$$

and we use the parametrization

$$\begin{cases} Z_1 = \tilde{\tau} \left( \frac{1}{2} - x \right) \\ Z_2 = \tilde{\tau} \left( \frac{1}{2} + x \right) \end{cases}, \quad \begin{cases} \tilde{z}_0^{(1)} = \frac{\tilde{\tau}}{2} + \left( \frac{1}{2} + y \right) \\ z_0^{(2)} = \frac{\tilde{\tau}}{2} + \left( \frac{1}{2} - y \right) \end{cases}. \quad (3.22)$$

Since  $z_0^{(1)} + 2\tilde{\tau}$  and  $z_0^{(1)}$  on the  $u$  plane correspond to a single point  $\rho_0^{(1)}$  on the  $\rho$  plane, we find, using the period  $\tilde{\tau} + 1/2$  of  $\rho(u)$ ,

$$0 = \rho(z_0^{(1)} + 2\tilde{\tau}) - \rho(z_0^{(1)}) = \rho(z_0^{(1)} + 2(\tilde{\tau} + \frac{1}{2}) - 1) - \rho(z_0^{(1)})$$

$$\begin{aligned}
&= 4\pi i\alpha_1(Z_1 - Z_2) + A(2(\tilde{\tau} + \frac{1}{2}) - 1) = -8\pi i\alpha_1\tilde{\tau}x + 2\tilde{\tau}A \\
\Rightarrow \quad A &= 4\pi i\alpha_1x.
\end{aligned} \tag{3.23}$$

Then,  $2\pi i\alpha_1(Z_1 - Z_2) = -\tilde{\tau}A$ , and hence the periodicity relation (3.2) can be rewritten as

$$\rho(u + m(\tilde{\tau} + \frac{1}{2}) + n) - \rho(u) = A\left(\frac{m}{2} + n\right). \tag{3.24}$$

Using this periodicity and Eq. (3.21), we obtain

$$\begin{aligned}
A &= \rho(\tilde{z}_0^{(1)}) - \rho(\hat{z}_0^{(2)}) = \rho(z_0^{(1)} + (\tilde{\tau} + \frac{1}{2})) - \rho(\hat{z}_0^{(2)}) \\
&= \rho_0^{(1)} + \frac{A}{2} - \rho_0^{(2)*} = i(\sigma_1 + \sigma_2) + \frac{A}{2} \\
\Rightarrow \quad \sigma_1 + \sigma_2 &= 2\pi\alpha_1x
\end{aligned} \tag{3.25}$$

and also

$$\begin{aligned}
i(\sigma_2 - \sigma_1) &= \rho(z_0^{(2)}) - \rho(z_0^{(1)}) = \rho(z_0^{(2)}) - \rho(\tilde{z}_0^{(1)} - (\tilde{\tau} + \frac{1}{2})) \\
&= \rho(z_0^{(2)}) - \rho(\tilde{z}_0^{(1)}) + \frac{A}{2} \\
&= 2\alpha_1 \ln \frac{\vartheta_1(\tilde{z}_0^{(1)} - Z_2|\tilde{\tau} + \frac{1}{2})}{\vartheta_1(\tilde{z}_0^{(1)} - Z_1|\tilde{\tau} + \frac{1}{2})} + A(z_0^{(2)} - \tilde{z}_0^{(1)}) + \frac{A}{2} \\
\Rightarrow \quad i \frac{\sigma_2 - \sigma_1}{\alpha_1} &= -2 \ln \frac{\vartheta_2(\tilde{\tau}x + y|\tilde{\tau} + \frac{1}{2})}{\vartheta_2(\tilde{\tau}x - y|\tilde{\tau} + \frac{1}{2})} + 2\pi i x(1 - 4y).
\end{aligned} \tag{3.26}$$

The equation determining the interaction point  $y$  is again the same as the stationarity condition  $\partial(\sigma_1 - \sigma_2)/\partial y = 0$ :

$$g_2(\tilde{\tau}x + y|\tilde{\tau} + \frac{1}{2}) + g_2(\tilde{\tau}x - y|\tilde{\tau} + \frac{1}{2}) = -4\pi i x. \tag{3.27}$$

### 3.5. $UU$ diagram

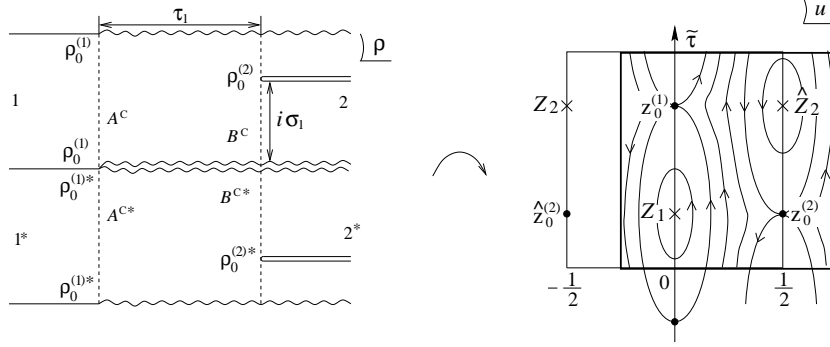
The diagram obtained by using  $U$  vertex twice is again a tree diagram from the SFT viewpoint but is a one-loop diagram from the CFT viewpoint. The mapping of the  $UU$  diagram to torus is drawn in Fig. 9. The period  $\tau$  in this case is  $\tilde{\tau}$ , the same as in planar case, and we parametrize the positions of punctures and interaction points as

$$\begin{cases} Z_1 = \tilde{\tau} \left( \frac{1}{2} - x \right) \\ Z_2 = -\frac{1}{2} + \tilde{\tau} \left( \frac{1}{2} + x \right) \end{cases}, \quad \begin{cases} z_0^{(1)} = \tilde{\tau} \left( \frac{1}{2} + y \right) \\ z_0^{(2)} = \frac{1}{2} + \tilde{\tau} \left( \frac{1}{2} - y \right) \end{cases}. \tag{3.28}$$

From periods  $\tilde{\tau}$  and 1, we obtain

$$\begin{aligned}
\pi i\alpha_1 &= \rho(z_0^{(1)}) - \rho(z_0^{(1)} - \tilde{\tau}) = 2\pi i\alpha_1(Z_1 - Z_2) + A\tilde{\tau} \\
\Rightarrow \quad A &= 4\pi i\alpha_1x,
\end{aligned} \tag{3.29}$$

$$\begin{aligned}
2i\sigma_1 &= \rho(z_0^{(2)}) - \rho(\hat{z}_0^{(2)}) = \rho(\hat{z}_0^{(2)} + 1) - \rho(\hat{z}_0^{(2)}) = A \\
\Rightarrow \quad \sigma_1 &= 2\pi\alpha_1x.
\end{aligned} \tag{3.30}$$

Fig. 9. Conformal mapping of the  $\rho$  plane of  $UU$  diagram to a torus.

As for the relation between  $\tau_1$  and the torus moduli  $\tilde{\tau}$ , we find

$$\begin{aligned}
 \tau_1 + i\sigma_1 &= \rho(z_0^{(2)}) - \rho(z_0^{(1)} - \tilde{\tau}) = \rho(z_0^{(2)}) - \rho(z_0^{(1)}) + \pi i\alpha_1 \\
 &= 2\alpha_1 \ln \frac{\vartheta_1(z_0^{(1)} - Z_2|\tilde{\tau})}{\vartheta_1(z_0^{(1)} - Z_1|\tilde{\tau})} + A(z_0^{(2)} - z_0^{(1)}) + \pi i\alpha_1 \\
 \Rightarrow \frac{\tau_1}{\alpha_1} &= -2 \ln \frac{\vartheta_1(\tilde{\tau}(x+y)|\tilde{\tau})}{\vartheta_2(\tilde{\tau}(x-y)|\tilde{\tau})} - 8\pi i x \tilde{\tau} y + \pi i. \tag{3.31}
 \end{aligned}$$

Stationarity  $\partial\tau_1/\partial y = 0$  determines the interaction point  $y$ :

$$g_1(\tilde{\tau}(x+y)|\tilde{\tau}) + g_2(\tilde{\tau}(x-y)|\tilde{\tau}) = -4\pi i x. \tag{3.32}$$

#### §4. Jacobian

In the explicit computation of the amplitudes below, we will need to make change of the variables from the moduli parameters on the  $\rho$  plane to the torus moduli  $\tau$  and  $x$ . Here we compute the Jacobian for this change of variables, for each case of the diagrams.

##### 4.1. general

Since the Jacobi  $\vartheta$  functions satisfy

$$\frac{\partial \vartheta_i(\nu|\tau)}{\partial \tau} = -\frac{i}{4\pi} \frac{\partial^2 \vartheta_i(\nu|\tau)}{\partial \nu^2}, \tag{4.1}$$

we have the following relation using  $g_i(\nu|\tau)$  defined in Eq. (3.4):

$$\frac{\partial}{\partial \tau} \ln \vartheta_i(\nu|\tau) = -\frac{i}{4\pi} \frac{\vartheta_i''}{\vartheta_i}(\nu|\tau) = -\frac{i}{4\pi} (g_i' + g_i^2)(\nu|\tau). \tag{4.2}$$

Using this equation, we can  $\tau$ -differentiate Eq.(3.1) with  $u$  generally dependent of  $\tau$ :

$$\frac{\partial \rho(u)}{\partial \tau} = \frac{\partial u}{\partial \tau} \frac{d\rho}{du} - \sum_{r=1,2} \alpha_r \frac{\partial Z_r}{\partial \tau} g_1(u - Z_r) - \sum_{r=1,2} \frac{i\alpha_r}{4\pi} \left( g_1'(u - Z_r) + g_1^2(u - Z_r) \right), \tag{4.3}$$

where the period  $\tau$  has been omitted for brevity. When  $u = z_0^{(i)}$  (in the fundamental region),  $d\rho/du(z_0^{(i)}) = 0$  because of Eq. (3.5) and we have

$$\frac{\partial \rho(z_0^{(i)})}{\partial \tau} = - \sum_{r=1,2} \alpha_r \frac{\partial Z_r}{\partial \tau} g_1(z_0^{(i)} - Z_r) - \sum_{r=1,2} \frac{i\alpha_r}{4\pi} \left( g_1'(z_0^{(i)} - Z_r) + g_1^2(z_0^{(i)} - Z_r) \right). \quad (4.4)$$

Using further the identities

$$\begin{aligned} \vartheta_1(z_0^{(2)} - Z_1) &= \vartheta_1(z_0^{(1)} - Z_2) \quad \text{when } Z_1 + Z_2 + 1 = z_0^{(1)} + z_0^{(2)} \\ \Rightarrow g_1(z_0^{(2)} - Z_1) &= -g_1(z_0^{(1)} - Z_2), \quad g_1'(z_0^{(2)} - Z_1) = g_1'(z_0^{(1)} - Z_2), \end{aligned} \quad (4.5)$$

where  $z_0^{(1)}$  is understood to be  $\tilde{z}_0^{(1)}$  for the  $V_\infty$  case, we obtain

$$\begin{aligned} &\frac{\partial}{\partial \tau} \left( \rho(z_0^{(2)}) - \rho(z_0^{(1)}) \right) \\ &= \alpha_1 \frac{\partial(Z_1 - Z_2)}{\partial \tau} \left( g_1(z_0^{(1)} - Z_1) + g_1(z_0^{(1)} - Z_2) \right) \\ &\quad + \frac{i\alpha_1}{2\pi} \left( g_1'(z_0^{(1)} - Z_1) - g_1'(z_0^{(1)} - Z_2) + g_1^2(z_0^{(1)} - Z_1) - g_1^2(z_0^{(1)} - Z_2) \right) \\ &= \frac{i\alpha_1}{2\pi} \left( g_1(z_0^{(1)} - Z_1) + g_1(z_0^{(1)} - Z_2) \right) \left\{ g_1(z_0^{(1)} - Z_1) - g_1(z_0^{(1)} - Z_2) - 2\pi i \frac{\partial(Z_1 - Z_2)}{\partial \tau} \right\} \\ &\quad + \frac{i\alpha_1}{2\pi} \left[ g_1'(z_0^{(1)} - Z_1) - g_1'(z_0^{(1)} - Z_2) \right]. \end{aligned} \quad (4.6)$$

In the present case of tachyon amplitude, we shall see below that the amplitudes for P, NO (M1 and M2) and NP diagrams contain delta function factor  $\delta(\tau_1 - \tau_2)$  (which is always the case when the external string states have no excitations of  $\alpha_n^-$  modes (See §7)). Then, as seen in Eqs. (3.9), (3.13) and (3.18) in those cases of P, NO (M1 and M2) and NP diagrams,  $\tau_1 = \tau_2$  means

$$A = 2\pi i \alpha_F = 4\pi i \alpha_1 x, \quad (4.7)$$

the same expression as Eqs. (3.23) and (3.29) for the  $V_\infty$  and  $UU$  amplitude cases. Thus, for all amplitude cases, we have

$$-2\pi i \frac{\partial(Z_1 - Z_2)}{\partial \tau} = 4\pi i x = \frac{A}{\alpha_1}, \quad (4.8)$$

which together with Eq.(3.5) implies that the part enclosed by a curly bracket in Eq. (4.6) vanishes. Consequently we obtain

$$\frac{\partial}{\partial \tau} \left( \rho(z_0^{(2)}) - \rho(z_0^{(1)}) \right) = \frac{i\alpha_1}{2\pi} \left[ g_1'(z_0^{(1)} - Z_1|\tau) - g_1'(z_0^{(1)} - Z_2|\tau) \right]. \quad (4.9)$$

#### 4.2. P, NO, NP

In these cases under the condition  $\tau_1 = \tau_2$ , remaining two free parameters are

$$\begin{aligned} \alpha_F &= 2\alpha_1 x, \\ \tau_1 &= \begin{cases} \rho(z_0^{(2)}) - \rho(z_0^{(1)}) & \text{for P, NO} \\ \rho(z_0^{(2)}) - \rho(z_0^{(1)}) - \pi i \alpha_1 + 2\pi i \alpha_1 x & \text{for NP} \end{cases}. \end{aligned} \quad (4.10)$$

Taking account of Eq.(4·9), the Jacobian for the change of variables  $(\tau_1, \alpha_F) \rightarrow (\tau, x)$  has the form

$$\begin{aligned} d\tau_1 d\alpha_F &= \frac{\partial(\tau_1, \alpha_F)}{\partial(\tau, x)} d\tau dx = \frac{\partial\tau_1}{\partial\tau} \frac{\partial\alpha_F}{\partial x} d\tau dx \\ &= 2\alpha_1 \cdot \frac{i\alpha_1}{2\pi} \left[ g'_1(z_0^{(1)} - Z_1|\tau) - g'_1(z_0^{(1)} - Z_2|\tau) \right] d\tau dx. \end{aligned} \quad (4\cdot11)$$

Here  $\tau = \tilde{\tau}$  for P, NP and  $\tau = \tilde{\tau} + \frac{1}{2}$  for NO, but  $d\tau = d\tilde{\tau}$  in any case. More explicitly, using Eqs. (3·7), (3·16),  $g_1(u + 1/2) = g_2(u)$  and  $g'_i(-u) = g'_i(u)$ ,

$$d\tau_1 d\alpha_F = -\frac{i\alpha_1^2}{\pi} \times \begin{cases} \left[ g'_2(\tilde{\tau}(x+y)|\tilde{\tau}) - g'_2(\tilde{\tau}(x-y)|\tilde{\tau}) \right] d\tilde{\tau} dx & \text{for P} \\ \left[ g'_2\left(\tilde{\tau}(x+y)|\tilde{\tau} + \frac{1}{2}\right) - g'_2\left(\tilde{\tau}(x-y)|\tilde{\tau} + \frac{1}{2}\right) \right] d\tilde{\tau} dx & \text{for NO} \\ \left[ g'_1(\tilde{\tau}(x+y)|\tilde{\tau}) - g'_2(\tilde{\tau}(x-y)|\tilde{\tau}) \right] d\tilde{\tau} dx & \text{for NP} \end{cases} \quad (4\cdot12)$$

#### 4.3. $V_\alpha$

Two free parameters in this  $V_\alpha$  case are

$$\begin{aligned} i\sigma_+ &\equiv i(\sigma_1 + \sigma_2) = 2\pi i\alpha_1 x \\ i\sigma_- &\equiv i(\sigma_2 - \sigma_1) = \rho(z_0^{(2)}) - \rho(\tilde{z}_0^{(1)}) + 2\pi i\alpha_1 x. \end{aligned} \quad (4\cdot13)$$

The Jacobian for the change of variables  $(\sigma_1, \sigma_2) \rightarrow (\tau, x)$  is given by

$$\begin{aligned} d\sigma_1 d\sigma_2 &= -\frac{1}{2} d\sigma_- d\sigma_+ = \frac{1}{2} \frac{\partial(i\sigma_-, i\sigma_+)}{\partial(\tau, x)} d\tau dx = \frac{1}{2} \frac{\partial i\sigma_-}{\partial\tau} \frac{\partial i\sigma_+}{\partial x} d\tau dx \\ &= i\pi\alpha_1 \cdot \frac{i\alpha_1}{2\pi} \left[ g'_1(\tilde{z}_0^{(1)} - Z_1|\tau) - g'_1(\tilde{z}_0^{(1)} - Z_2|\tau) \right] d\tau dx. \end{aligned} \quad (4\cdot14)$$

More explicitly, using  $\tau = \tilde{\tau} + 1/2$  and Eq. (3·22),

$$d\sigma_1 d\sigma_2 = -\frac{\alpha_1^2}{2} \left[ g'_2\left(\tilde{\tau}x + y|\tilde{\tau} + \frac{1}{2}\right) - g'_2\left(\tilde{\tau}x - y|\tilde{\tau} + \frac{1}{2}\right) \right] d\tilde{\tau} dx. \quad (4\cdot15)$$

#### 4.4. $UU$

Free parameters in the  $UU$  case are

$$\begin{aligned} \sigma_1 &= 2\pi\alpha_1 x \\ \tau_1 &= \rho(z_0^{(2)}) - \rho(z_0^{(1)}) + \pi i\alpha_1 - 2\pi i\alpha_1 x, \end{aligned} \quad (4\cdot16)$$

so that the Jacobian for the change of variables  $(\sigma_1, \tau_1) \rightarrow (\tau, x)$  reads

$$\begin{aligned} d\tau_1 d\sigma_1 &= \frac{\partial(\tau_1, \sigma_1)}{\partial(\tau, x)} d\tau dx = \frac{\partial\tau_1}{\partial\tau} \frac{\partial\sigma_1}{\partial x} d\tau dx \\ &= 2\pi\alpha_1 \cdot \frac{i\alpha_1}{2\pi} \left[ g'_1(z_0^{(1)} - Z_1|\tau) - g'_1(z_0^{(1)} - Z_2|\tau) \right] d\tau dx. \end{aligned} \quad (4\cdot17)$$

More explicitly, using  $\tau = \tilde{\tau}$  and Eq. (3·28),

$$d\tau_1 d\sigma_1 = i\alpha_1^2 \left[ g'_1(\tilde{\tau}(x+y)|\tilde{\tau}) - g'_2(\tilde{\tau}(x-y)|\tilde{\tau}) \right] d\tilde{\tau} dx. \quad (4\cdot18)$$



## §5. CFT correlation functions on the torus

### 5.1. Correlation functions and GGRT

To compute the CFT correlation functions on the torus, we further map the  $u$  plane to the  $\tilde{\rho} = -2\pi i u$  plane such that the  $\tilde{\rho} = \tau + i\sigma$  plane becomes of the usual open string strip with  $\text{Im}\tilde{\rho} (= \sigma) = 0$  and  $\pi$  being the open string boundaries and, therefore, the usual Fourier expansion  $\phi(\tilde{\rho}) = \sum_n \phi_n e^{-n\tilde{\rho}}$  can be used there for the string coordinate and ghost fields  $\phi = X, b$  and  $c$ . Then, the CFT correlation functions can be calculated by the following formulas: for the cases of P and NP diagrams with period  $\tilde{\tau}$ ,

$$\left\langle \prod_r \mathcal{O}_r(u_r) \right\rangle_{\tilde{\tau}} = (-2\pi i)^{\sum_r d_r} \text{Tr} \left[ (-)^{N_{\text{FP}}+1} w^{(L_0-c/24)} \prod_r \mathcal{O}_r(-2\pi i u_r) \right], \quad (5.1)$$

and for the NO (M1 and M2) cases with period  $\tilde{\tau} + \frac{1}{2}$ ,

$$\left\langle \prod_r \mathcal{O}_r(u_r) \right\rangle_{\tilde{\tau}+\frac{1}{2}} = (-2\pi i)^{\sum_r d_r} \text{Tr} \left[ \Omega(-)^{N_{\text{FP}}+1} w^{(L_0-c/24)} \prod_r \mathcal{O}_r(-2\pi i u_r) \right], \quad (5.2)$$

where  $w \equiv e^{2\pi i \tilde{\tau}}$ ,  $N_{\text{FP}}$  is the ghost number operator (whose explicit expression is given shortly),  $c$  is the central charge of the system, and  $\Omega$  is the (open string) twist operator,  $\Omega : u \rightarrow u + \frac{1}{2}$  ( $\tilde{\rho} \rightarrow \tilde{\rho} - \pi i$ ). Here we have assumed that the operators  $\mathcal{O}_r$  are *primary fields* with conformal weights  $d_r$ , as being always the case in our computations below.

As noted before, these formulas are *not* mere definitions of the torus CFT correlation functions but the result of the GGRT<sup>13)</sup> for the cases of P, NP and NO diagrams. Actually, once the period is specified, the functional form of the torus correlation function is unique but the overall normalization factor is *not*. GGRT determines those normalization factors also.

For the remaining  $UU$  and  $V_\infty$  cases, these formula does not give the correct normalization factor. First consider the  $UU$  diagram case, in which the  $\langle v_{UU} |$  vertex is given in Eq. (2.12) by contracting two tree level  $U$  vertices by closed reflector  $|R^c(A^c, B^c)\rangle$ . In view of the  $u$  plane in Fig. 9 in which the vertical lines represent the intermediate closed string, we note that the direction of the time evolution on the  $u$  plane is not vertical but horizontal in the  $UU$  diagram case. So the trace operation should be taken in the horizontal direction in this  $UU$  diagram case, and the correct mapping from the  $u$  plane to  $\tilde{\rho}$  plane should be  $\tilde{\rho} = 2\pi u(i/\tilde{\tau}) + \text{const.}$  such that the image of the vertical line  $\text{Re}u = \text{const.}$ ,  $0 \leq \text{Im}u \leq |\tilde{\tau}|$  ( $= \tilde{\tau}/i$ ) has the correct width  $2\pi$  in  $\sigma = \text{Im}\tilde{\rho}$ . Using this mapping and denoting  $-1/\tilde{\tau} \equiv \tau$ , the correct formula in this  $UU$  case reads

$$\left\langle \prod_r \mathcal{O}_r(u_r) \right\rangle_{UU, \tau} = (-2\pi i \tau)^{\sum_r d_r} \text{Tr}' \left[ (-)^{N_{\text{FP}}+1} q^{2(L_0-c/24)} \prod_r \mathcal{O}_r(-2\pi i \tau u_r) \right], \quad (5.3)$$

where  $q \equiv e^{\pi i \tau}$ , and  $\text{Tr}'$  means that no trace is taken over the momentum; the ‘trace’  $\text{Tr}_0[\cdots]$  in the zero mode sector of  $X$  is simply  $\langle -k_1/2 | \cdots | -k_1/2 \rangle$  where  $k_1$  is the momentum of the external string 1. We emphasize again that the difference between

the CFT correlation functions (5.1) and (5.3) computed vertically and horizontally, respectively, in fact appears only in their numerical coefficients and their function forms are exactly the same.

For completeness, we present here the proof for this formula (5.3). It can be proven by using the GGRT for the case of open-string loop diagram.<sup>13)</sup> The closed string  $A^c$  can be treated essentially as a product of two open strings  $A$  and  $\bar{A}$ , corresponding to the holomorphic and anti-holomorphic pieces. This identification is, however, slightly violated in the zero-mode sector of  $X$ , since there exists only a single zero-mode  $x$  (or  $p$ ) common to the holomorphic and anti-holomorphic parts. To make the identification exact, we can extend the zero mode sector such that both the holomorphic and anti-holomorphic sectors have their own zero modes  $p$  and  $\bar{p}$ , and identify the original state  $|p_1\rangle$  to be  $|p, \bar{p}\rangle$  with  $p + \bar{p} = p_1$  and  $p - \bar{p} = 0$ . Then, taking account of  $dp d\bar{p} = d(p + \bar{p}) d((p - \bar{p})/2)$ , we can identify the closed reflector  $|R^c(A^c, B^c)\rangle$  as

$$|R^c(A^c, B^c)\rangle = (2\pi)^d \delta^d\left(\frac{\hat{p}_A - \hat{p}_{\bar{A}}}{2}\right) |R^o(A, B)\rangle |R^o(\bar{A}, \bar{B})\rangle \quad (5.4)$$

and the vertex  $\langle u(1, A^c)|$ , for instance, becomes to have momentum conservation factor  $\delta^d(p_A + \bar{p}_A + k_1)$  instead of  $\delta^d(p_A + k_1)$ . With this device, we now apply the GGRT<sup>8), 13)</sup> for the open string case to the present  $UU$  vertex contracted by the closed string reflector: with  $\rho_1 \equiv \tau_1 + i\sigma_1$ ,

$$\begin{aligned} & \langle v_{UU}(\tau_1, \sigma_1)| \\ &= \langle u(1, A^c)| \langle u(2, B^c)| e^{-L_0 \rho_1} e^{-\bar{L}_0 \bar{\rho}_1} |R^c(A^c, B^c)\rangle \\ &= \langle u(\bar{A}, 1, A)| e^{-L_0 \rho_1} \langle u(B, 2, \bar{B})| e^{-\bar{L}_0 \bar{\rho}_1} (2\pi)^d \delta^d\left(\frac{\hat{p}_A - \hat{p}_{\bar{A}}}{2}\right) |R^o(A, B)\rangle |R^o(\bar{A}, \bar{B})\rangle \\ &= \langle u(\bar{A}, 1, A)| e^{-L_0 \rho_1} \langle u(B, 2, \bar{B})| |R^o(A, B)\rangle e^{-\bar{L}_0 \bar{\rho}_1} (2\pi)^d \delta^d\left(\hat{p}_{\bar{A}} + \frac{k_1}{2}\right) |R^o(\bar{A}, \bar{B})\rangle \\ &= \langle v(\bar{A}, 1, 2, \bar{B})| e^{-\bar{L}_0 \bar{\rho}_1} (2\pi)^d \delta^d\left(\hat{p}_{\bar{A}} + \frac{p_1}{2}\right) |R^o(\bar{A}, \bar{B})\rangle, \end{aligned} \quad (5.5)$$

where we have used the momentum conservation  $\langle u(\bar{A}, 1, A)| (\hat{p}_A + \hat{p}_{\bar{A}} + k_1) = 0$  in going to the third expression, and the tree level GGRT  $\langle v(\bar{A}, 1, 2, \bar{B})| = \langle u(\bar{A}, 1, A)| e^{-L_0 \rho_1} \langle u(B, 2, \bar{B})| |R(A, B)\rangle$  in going to the last line. Since every quantities are now of open-string, we can apply the loop level GGRT proven in Ref. 13) to the last expression and obtain

$$\begin{aligned} & \langle v_{UU}(\tau_1, \sigma_1)| |\Phi_2\rangle |\Phi_1\rangle \\ &= \int \frac{d^d p}{(2\pi)^d} \langle p| (2\pi)^d \delta^d\left(\hat{p}_{\bar{A}} + \frac{k_1}{2}\right) \text{Tr}_{n \neq 0} \left[ (-)^{N_{\text{FP}}+1} q^{2L_0} \prod_i h_i[\Phi_i] \right] |p\rangle \\ &= \left\langle -\frac{k_1}{2} \left| \text{Tr}_{n \neq 0} \left[ (-)^{N_{\text{FP}}+1} q^{2L_0} \prod_i h_i[\Phi_i] \right] \right| -\frac{k_1}{2} \right\rangle. \end{aligned} \quad (5.6)$$

Note that the bra and ket zero-mode states here correspond to the ‘open strings’ of anti-holomorphic parts  $\bar{B}$  and  $\bar{A}$ , respectively. Therefore this expression corresponds

to the cutting of the torus on the  $u$  plane as indicated by bold line in Fig. 9, and also shows that the time evolution direction is horizontal as claimed above.

Finally, consider the  $V_\infty$  case. Actually we have not given a precise definition of the  $\langle v_\infty |$  vertex in the preceding papers I and II, since it refers to CFT on the torus. Nevertheless, we have used in I the GGRT that the two glued vertices

$$\begin{aligned} \langle v_1(1, 4^c; \sigma_0, \theta, \tau) | &\equiv \langle u(1, 2^c) | \langle v_\infty(3^c, 4^c; \sigma_0) | e^{-\tau(L+\bar{L})} e^{i\theta(L-\bar{L})} | R^c(2^c, 3^c) \rangle , \\ \langle v_2(1, 4^c; \sigma_1, \sigma_2, \tau) | &\equiv - \langle v_\infty(1, 2; \sigma_1, \sigma_2) | \langle u(3, 4^c) | e^{-\tau L} | R^o(2, 3) \rangle , \end{aligned} \quad (5.7)$$

become identical at  $\tau = 0$ . Since  $\langle v_\infty |$  and  $\langle u |$  are already defined, this identity fixes the normalization of the  $\langle v_\infty |$  vertex. The minus sign in the expression of  $\langle v_2 |$  here is because the contraction was taken by  $|R^o(3, 2)\rangle = -|R^o(2, 3)\rangle$  in I. However, the contraction by  $|R^o(2, 3)\rangle$  is more natural in the sign from the GGRT view point, so we here require that  $\langle v_1(1, 4^c; \sigma_0, \theta, \tau) | = - \langle v_2(1, 4^c; \sigma_1, \sigma_2, \tau) |$  holds at  $\tau = 0$  by changing the sign convention of the  $\langle v_\infty |$  vertex and hence of the coupling constant  $x_u$  from I and II. In order for this identity to hold, the  $\langle v_\infty |$  vertex should be defined by referring to the ‘horizontal’ computation as in the  $UU$  case. Indeed the first glued vertex  $\langle v_1 |$  is given by contraction using the closed string reflector  $|R^c(2^c, 3^c)\rangle$  which contains the delta function constraining the intermediate state momentum as in Eq. (5.4). To perform horizontal calculation, we note that the ‘vertical’ period  $\tilde{\tau} + 1/2$  is equivalent to the ‘horizontal’ period

$$\frac{1 - (\tilde{\tau} + 1/2)}{1 - 2(\tilde{\tau} + 1/2)} = \frac{\tau}{4} + \frac{1}{2}, \quad (5.8)$$

which corresponds to taking the torus fundamental region to be the region enclosed by the dotted bold line in Fig. 8, and the fundamental region on the  $u$  plane is mapped to  $\tilde{\rho}$ -plane by  $\tilde{\rho} = 2\pi i u / 2\tilde{\tau} + \text{const.} = -\pi i \tau u + \text{const.}$  such that the image of the vertical line  $\text{Re} u = -y$ ,  $-|\tilde{\tau}|/2 \leq \text{Im} u \leq 3|\tilde{\tau}|/2$  has the correct width  $2\pi$  in  $\sigma = \text{Im} \tilde{\rho}$ . Using this mapping, the correct formula for defining the  $V_\infty$  vertex is:

$$\begin{aligned} \left\langle \prod_r \mathcal{O}_r(u_r) \right\rangle_{V_\infty, \frac{\tau}{4} + \frac{1}{2}} \\ = (-\pi i \tau) \sum_r d_r \langle 0 | \text{Tr}_{n \neq 0} \left[ \Omega(-)^{N_{\text{FP}}+1} q^{\frac{1}{2}(L_0 - c/24)} \prod_r \mathcal{O}_r(-\pi i \tau u_r) \right] | 0 \rangle , \end{aligned} \quad (5.9)$$

where  $q \equiv e^{\pi i \tau}$ , and  $\langle 0 | \cdots | 0 \rangle$  means that the expectation value is taken with momentum 0 state in the zero mode sector of  $X$ . If we have adopted the ‘vertical’ definition (5.2) for this case also, the weight would be different by an intriguing factor  $2^{d/2}/(2\pi)^{d_i}$ :

$$\left\langle \prod_r \mathcal{O}_r(u_r) \right\rangle_{\tilde{\tau} + \frac{1}{2}} = \frac{2^{d/2}}{(2\pi)^{d_i}} \left\langle \prod_r \mathcal{O}_r(u_r) \right\rangle_{V_\infty, \frac{\tau}{4} + \frac{1}{2}} \quad (5.10)$$

for the operator  $\prod_r \mathcal{O}_r(u_r) = b_{\sigma_1} b_{\sigma_2} c(Z_2) e^{ik_2 \cdot X(Z_2)} c(Z_1) e^{ik_1 \cdot X(Z_1)}$  relevant here, as we shall see below.

Let us now evaluate the ghost and  $X$  parts, separately.

### 5.2. ghost part

As is seen in Eqs. (2·8), (2·13) and (2·14), the correlation functions we need in this paper have the following form as their ghost parts:

$$\langle b(u_1)b(u_2)c(Z_2)c(Z_1) \rangle_J \quad \text{where} \quad J = \begin{cases} \tilde{\tau} & \text{for P and NP} \\ \tilde{\tau} + \frac{1}{2} & \text{for NO (M1, M2)} \\ \tau & \text{for } UU \\ \frac{\tau}{4} + \frac{1}{2} & \text{for } V_\infty \end{cases} \quad (5.11)$$

#### 5.2.1. P and NP

First consider the planar and nonplanar diagram cases with period  $\tilde{\tau}$ , to which the formula (5.1) applies. Substituting into it the expansion of the ghost fields on the  $\tilde{\rho} = -2\pi i u$  plane

$$c(\tilde{\rho}) = \sum_n c_n e^{-n\tilde{\rho}}, \quad b(\tilde{\rho}) = \sum_n b_n e^{-n\tilde{\rho}}, \quad (5.12)$$

we evaluate the ghost correlation function as follows:\*

$$\begin{aligned} \langle b(u_1)b(u_2)c(Z_2)c(Z_1) \rangle_{\tilde{\tau}} &= \langle b(u_2)c(Z_2)b(u_1)c(Z_1) \rangle_{\tilde{\tau}} \\ &= (-2\pi i)^{2 \cdot 2 - 2 \cdot 1} \text{Tr} \left[ (-)^{N_{\text{FP}}+1} w^{(L_0^{\text{FP}} + \frac{1}{12})} b(-2\pi i u_2) c(-2\pi i Z_2) b(-2\pi i u_1) c(-2\pi i Z_1) \right] \\ &= -(2\pi i)^2 w^{\frac{1}{12}} \text{Tr} \left[ (-)^{N_{\text{FP}}} w^{L_0^{\text{FP}}} \left\{ b_0 c_0 b_0 c_0 + \sum_{n \neq 0} \left( b_0 c_0 b_n c_{-n} e^{2\pi i n(u_1 - Z_1)} \right. \right. \right. \\ &\quad \left. \left. \left. + b_0 c_0 c_{-n} b_n e^{2\pi i n(u_1 - Z_2)} + c_0 b_0 b_n c_{-n} e^{2\pi i n(u_2 - Z_1)} + b_0 c_0 b_n c_{-n} e^{2\pi i n(u_2 - Z_2)} \right) \right\} \right], \quad (5.13) \end{aligned}$$

where use has been made of the ghost central charge  $c_{\text{FP}} = -26$  and

$$\begin{aligned} N_{\text{FP}} &= c_0 b_0 + \sum_{n \geq 1} (c_{-n} b_n - b_{-n} c_n), \\ L_0^{\text{FP}} &= \sum_{n \geq 1} n (c_{-n} b_n + b_{-n} c_n) = L_{0\text{CFT}}^{\text{FP}} + 1. \end{aligned} \quad (5.14)$$

The trace  $\text{Tr}$  can be calculated mode by mode,  $\text{Tr} = \text{Tr}_0 \times \prod_{n=1}^{\infty} \text{Tr}_n$ . Noting, in particular, the zero-mode part trace formula  $\text{Tr}_0[(-)^{N_{\text{FP}}} b_0 c_0] = -\text{Tr}_0[(-)^{N_{\text{FP}}} c_0 b_0] = 1$  and  $\text{Tr}_0[(-)^{N_{\text{FP}}} 1] = \text{Tr}_0[(-)^{N_{\text{FP}}} c_0] = \text{Tr}_0[(-)^{N_{\text{FP}}} b_0] = 0$ , as explained in Ref. 13), we obtain

$$\begin{aligned} \text{Tr} \left[ (-)^{N_{\text{FP}}} w^{L_0^{\text{FP}}} b_0 c_0 \right] &= [f(w)]^2 \quad \left( f(w) \equiv \prod_{n=1}^{\infty} (1 - w^n) \right) \\ \text{Tr} \left[ (-)^{N_{\text{FP}}} w^{L_0^{\text{FP}}} b_0 c_0 \sum_{l \neq 0} \left( \frac{b_l c_{-l}}{c_{-l} b_l} \right) e^{2\pi i l u} \right] &= [f(w)]^2 \left( \pm \frac{i}{2\pi} g_1(u|\tilde{\tau}) - \frac{1}{2} \right). \quad (5.15) \end{aligned}$$

---

\* Note that the time ordering is always implied in any CFT correlation functions. The operators are rearranged in the order of time in the first equation here.

Thus, together with the help of Eq. (3·3), the RHS of Eq. (5·13) reduces to

$$\begin{aligned} &= 2\pi i \left[ w^{\frac{1}{24}} f(w) \right]^2 \left\{ g_1(u_1 - Z_1 | \tilde{\tau}) - g_1(u_1 - Z_2 | \tilde{\tau}) - g_1(u_2 - Z_1 | \tilde{\tau}) + g_1(u_2 - Z_2 | \tilde{\tau}) \right\} \\ &= \frac{2\pi i}{\alpha_1} \left[ w^{\frac{1}{24}} f(w) \right]^2 \left\{ \frac{d\rho}{du}(u_1) - \frac{d\rho}{du}(u_2) \right\} \equiv \mathcal{G} \left\{ \frac{d\rho}{du}(u_1) - \frac{d\rho}{du}(u_2) \right\}. \end{aligned} \quad (5·16)$$

### 5.2.2. NO (M1 and M2)

Next we consider the nonorientable diagram case with period  $\tilde{\tau} + 1/2$ , to which the formula (5·2) applies. In this case, the twist operator  $\Omega$  is additionally inserted, and its effect can simply be taken into account by making replacements  $w \rightarrow -w$  and  $\tilde{\tau} \rightarrow \tilde{\tau} + 1/2$ . So we find\*

$$\begin{aligned} \text{Tr} \left[ \Omega(-)^{N_{\text{FP}}} w^{L_0^{\text{FP}}} b_0 c_0 \right] &= [f(-w)]^2, \\ \text{Tr} \left[ \Omega(-)^{N_{\text{FP}}} w^{L_0^{\text{FP}}} b_0 c_0 \sum_{l \neq 0} b_l c_{-l} e^{2\pi i l u} \right] &= [f(-w)]^2 \left( \frac{i}{2\pi} g_1(u | \tilde{\tau} + \frac{1}{2}) - \frac{1}{2} \right), \end{aligned} \quad (5·17)$$

etc., and hence

$$\begin{aligned} &\langle b(u_1) b(u_2) c(Z_2) c(Z_1) \rangle_{\tilde{\tau} + \frac{1}{2}} \\ &= 2\pi i \left[ w^{\frac{1}{24}} f(-w) \right]^2 \left\{ g_1(u_1 - Z_1 | \tilde{\tau} + \frac{1}{2}) - g_1(u_1 - Z_2 | \tilde{\tau} + \frac{1}{2}) \right. \\ &\quad \left. - g_1(u_2 - Z_1 | \tilde{\tau} + \frac{1}{2}) + g_1(u_2 - Z_2 | \tilde{\tau} + \frac{1}{2}) \right\} \\ &= \frac{2\pi i}{\alpha_1} \left[ w^{\frac{1}{24}} f(-w) \right]^2 \left\{ \frac{d\rho}{du}(u_1) - \frac{d\rho}{du}(u_2) \right\} \equiv \mathcal{G}^N \left\{ \frac{d\rho}{du}(u_1) - \frac{d\rho}{du}(u_2) \right\}. \end{aligned} \quad (5·18)$$

### 5.2.3. UU

Thirdly we consider the  $UU$  diagram case, to which the formula (5·3) applies. Comparing this formula with the previous one (5·1) for P and NP cases, we immediately see that we obtain the desired result in this case by making replacements  $w \rightarrow q^2$ ,  $u \rightarrow \tau u$  and  $(-2\pi i)^2 \rightarrow (-2\pi i \tau)^2$  (for the conformal factor) in the above first result (5·16):

$$\begin{aligned} &\langle b(u_1) b(u_2) c(Z_2) c(Z_1) \rangle_{\tau} \\ &= 2\pi i \tau^2 \left[ q^{\frac{1}{12}} f(q^2) \right]^2 \left\{ g_1(\tau(u_1 - Z_1) | \tau) - g_1(\tau(u_1 - Z_2) | \tau) \right. \\ &\quad \left. - g_1(\tau(u_2 - Z_1) | \tau) + g_1(\tau(u_2 - Z_2) | \tau) \right\}. \end{aligned} \quad (5·19)$$

But, the functions  $f$  and  $g_1$  have simple transformation properties under the Jacobi imaginary transformation  $\tau \rightarrow -1/\tau = \tilde{\tau}$ :

$$\left[ w^{\frac{1}{24}} f(w) \right]^2 = -i\tau \left[ q^{\frac{1}{12}} f(q^2) \right]^2, \quad g_1(\tau u | \tau) = \frac{1}{\tau} g_1(u | \tilde{\tau}) - 2\pi i u. \quad (5·20)$$

---

\* Note that the Fock vacuum  $|1\rangle \equiv c_1 |0\rangle$  is *even* under the twist  $\Omega$ ,  $\Omega |1\rangle = +|1\rangle$ , so  $SL(2; C)$  vacuum  $|0\rangle$  is *odd*.

Owing to these, the present correlation function (5.19) in fact turns out to equal the previous one (5.16) up to an overall factor  $i$ :

$$\langle b(u_1) b(u_2) c(Z_2) c(Z_1) \rangle_\tau = i \langle b(u_1) b(u_2) c(Z_2) c(Z_1) \rangle_{\bar{\tau}}. \quad (5.21)$$

This reflects the modular invariance of the theory, but note that the factor  $i$  difference remains here contrary to the vacuum energy.

#### 5.2.4. $V_\infty$

Final is the  $V_\infty$  diagram case, to which the formula (5.9) applies. Comparison of this formula with Eq. (5.2) for NO case shows that the result in this case can be obtained by making replacements  $w \rightarrow q^{1/2}$ ,  $u \rightarrow (\tau/2)u$  and  $(-2\pi i)^2 \rightarrow (-\pi i\tau)^2$  in the above result (5.18) for NO case:

$$\begin{aligned} & \langle b(u_1) b(u_2) c(Z_2) c(Z_1) \rangle_{\frac{\tau}{4} + \frac{1}{2}} \\ &= 2\pi i \left( \frac{\tau}{2} \right)^2 \left[ q^{\frac{1}{48}} f(-\sqrt{q}) \right]^2 \left\{ g_1\left(\frac{\tau}{2}(u_1 - Z_1) \middle| \frac{\tau}{4} + \frac{1}{2}\right) - g_1\left(\frac{\tau}{2}(u_1 - Z_2) \middle| \frac{\tau}{4} + \frac{1}{2}\right) \right. \\ & \quad \left. - g_1\left(\frac{\tau}{2}(u_2 - Z_1) \middle| \frac{\tau}{4} + \frac{1}{2}\right) + g_1\left(\frac{\tau}{2}(u_2 - Z_2) \middle| \frac{\tau}{4} + \frac{1}{2}\right) \right\}. \quad (5.22) \end{aligned}$$

Since the functions  $f$  and  $g_1$  have the following transformation laws under the modular transformation (5.8)

$$\left[ w^{\frac{1}{24}} f(-w) \right]^2 = -i \frac{\tau}{2} \left[ q^{\frac{1}{48}} f(-\sqrt{q}) \right]^2, \quad g_1\left(\frac{\tau}{2}u \middle| \frac{\tau}{4} + \frac{1}{2}\right) = \frac{2}{\tau} g_1(u | \tilde{\tau} + \frac{1}{2}) - 4\pi i u, \quad (5.23)$$

the present correlation function (5.22) again turns out to equal the previous one (5.18) up to a factor  $i$ :

$$\langle b(u_1) b(u_2) c(Z_2) c(Z_1) \rangle_{\frac{\tau}{4} + \frac{1}{2}} = i \langle b(u_1) b(u_2) c(Z_2) c(Z_1) \rangle_{\bar{\tau} + \frac{1}{2}}. \quad (5.24)$$

### 5.3. $X$ part

#### 5.3.1. covariant case

In our SFT, manifest Lorentz covariance is lost by the choice  $\alpha = (2)p^+$ . However, the violation occurs only in the zero mode  $p^\pm$  sector and all the other parts still retains the manifest covariance. So we first calculate the  $X$  correlation function in the manifest covariant case, and later will clarify where and how the covariant result is modified.

What we need calculate is the 2-point  $X$  correlation function:

$$\left\langle e^{ik_2 \cdot X(Z_2)} e^{ik_1 \cdot X(Z_1)} \right\rangle_{\bar{\tau}} = (-2\pi i)^{\frac{k_2^2}{2} + \frac{k_1^2}{2}} \text{Tr} \left[ w^{(L_0^X - \frac{d}{24})} : e^{ik_2 \cdot X(\tilde{\rho}_2)} : : e^{ik_1 \cdot X(\tilde{\rho}_1)} : \right], \quad (5.25)$$

where use has been made of the formula (5.1) and  $\tilde{\rho}_r = -2\pi i Z_r$  ( $r = 1, 2$ ). On the  $\tilde{\rho}$  plane, the coordinate fields  $X^\mu$  are expanded as

$$X^\mu(\tilde{\rho}) = x^\mu - i\alpha_0^\mu \tilde{\rho} + i \sum_{n \neq 0} \frac{1}{n} \alpha_n^\mu e^{-n\tilde{\rho}}, \quad (5.26)$$

and the normal ordered operator  $:e^{ik \cdot X(\tilde{\rho})}:$  is given by

$$:e^{ik \cdot X(\tilde{\rho})}: = e^{\frac{1}{2}\tilde{\rho}k^2} e^{ik \cdot \hat{x}} e^{\tilde{\rho}k \cdot \hat{p}} \prod_{n=1}^{\infty} e^{\frac{1}{n}k \cdot \alpha_{-n} e^{n\tilde{\rho}}} e^{-\frac{1}{n}k \cdot \alpha_n e^{-n\tilde{\rho}}}. \quad (5.27)$$

Note that  $e^{ik \cdot (x^\mu - i\alpha_0^\mu \tilde{\rho})} = e^{\frac{1}{2}\tilde{\rho}k^2} e^{ik \cdot \hat{x}} e^{\tilde{\rho}k \cdot \hat{p}}$  has been used. Inserting this into Eq. (5.25), we can evaluate the trace  $\text{Tr}$  part mode by mode,  $\text{Tr} = \text{Tr}_0 \times \prod_{n=1}^{\infty} \text{Tr}_n$ . Using

$$\begin{cases} \text{Tr}_0[\cdots] = \int \frac{d^d p}{(2\pi)^d} \langle p | \cdots | p \rangle \\ \text{Tr}_n[\cdots] = \int \frac{d^d z_n d^d \bar{z}_n}{\pi^d} e^{-|z_n|^2} \langle z_n | \cdots | z_n \rangle \end{cases} \quad (5.28)$$

(where  $\hat{p} |p\rangle = p |p\rangle$  normalized as  $\langle p | q \rangle = (2\pi)^d \delta^d(p - q)$ , and  $|z_n\rangle \equiv e^{z_n \cdot \alpha_{-n}/\sqrt{n}} |0\rangle$ ), we find

$$\text{Tr}_0[\cdots] = \delta^d(k_1 + k_2) w^{-\frac{d}{24}} \left( \frac{-2\pi}{\ln w} \right)^{\frac{d}{2}} \exp \left[ k_1 \cdot k_2 \left( \frac{(\tilde{\rho}_1 - \tilde{\rho}_2)^2}{2 \ln w} - \frac{\tilde{\rho}_1 - \tilde{\rho}_2}{2} \right) \right], \quad (5.29)$$

$$\prod_{n=1}^{\infty} \text{Tr}_n[\cdots] = \prod_{n=1}^{\infty} \frac{1}{(1 - w^n)^d} \exp \left[ -k_1 \cdot k_2 \left( \frac{e^{n(\tilde{\rho}_1 - \tilde{\rho}_2)} + w^n e^{-(\tilde{\rho}_1 - \tilde{\rho}_2)} - 2w^n}{n(1 - w^n)} \right) \right]. \quad (5.30)$$

Substituting these into Eq. (5.25), we obtain

$$\begin{aligned} & \left\langle e^{ik_2 \cdot X(Z_2)} e^{ik_1 \cdot X(Z_1)} \right\rangle_{\tilde{\tau}} \\ &= (-2\pi i)^{-k_1 \cdot k_2} \delta^d(k_1 + k_2) \left[ w^{\frac{1}{24}} f(w) \right]^{-d} \left( \frac{-2\pi}{\ln w} \right)^{\frac{d}{2}} \left[ \psi(e^{\tilde{\rho}_1 - \tilde{\rho}_2}, w) \right]^{k_1 \cdot k_2}, \end{aligned} \quad (5.31)$$

where  $\psi(\rho, w)$  is the function defined in Eq. (8.A.10) in GSW:<sup>12)</sup>

$$\psi(\rho, w) = \frac{1 - \rho}{\sqrt{\rho}} \exp \left( \frac{\ln^2 \rho}{2 \ln w} \right) \prod_{n=1}^{\infty} \frac{(1 - w^n \rho)(1 - w^n / \rho)}{(1 - w^n)^2}. \quad (5.32)$$

### 5.3.2. P, NP and NO cases

Let us see where and what modifications are necessary in our case of P, NP and NO diagrams.

First we should note that, in these cases of P, NP and NO diagrams, the loop momentum  $p$  in the zero-mode trace calculation  $\text{Tr}_0[\cdots]$ , Eq. (5.28), equals the minus of the momentum of the intermediate open string  $F$ , i.e.,  $p = -p_F$ ,<sup>\*</sup> and so  $-2p^+$  is just the string length  $\alpha_F$  of the string  $F$ . Since the conformal mappings to the torus for those cases *depend* on  $\alpha_F$ , the  $\alpha_F$  dependence appears everywhere not only in the zero-momentum trace part, so that the integration over  $\alpha_F$  cannot be performed in the zero-momentum trace part alone.

---

<sup>\*</sup> The minus sign is understandable if we note that the contours  $C$  and  $C'$  giving the zero modes  $p_F = i \oint_C (dw/2\pi i) \partial X(w)$  of string  $F$  and  $p = i \oint_{C'} (d\tilde{\rho}/2\pi i) \partial X(\tilde{\rho})$  on the  $\tilde{\rho}$  plane, have opposite directions by the mapping  $w \rightarrow \rho \rightarrow u \rightarrow \tilde{\rho}$ .

The zero-mode part of the trace  $\text{Tr}[w^{(L_0^X - \frac{d}{24})} : e^{ik_2 \cdot X(\tilde{\rho}_2)} :: e^{ik_1 \cdot X(\tilde{\rho}_1)} :]$  reads

$$\begin{aligned} & \text{Tr}_0 \left[ w^{(\frac{p^2}{2} - \frac{d}{24})} e^{ik_2 \cdot \hat{x}} e^{\tilde{\rho}_2 k_2 \cdot \hat{p}} e^{ik_1 \cdot \hat{x}} e^{\tilde{\rho}_1 k_1 \cdot \hat{p}} e^{\frac{1}{2}(\tilde{\rho}_1 k_1^2 + \tilde{\rho}_2 k_2^2)} \right] \\ &= \int \frac{d^d p}{(2\pi)^d} \langle p | w^{(\frac{p^2}{2} - \frac{d}{24})} e^{ik_2 \cdot \hat{x}} e^{\tilde{\rho}_2 k_2 \cdot \hat{p}} e^{ik_1 \cdot \hat{x}} e^{\tilde{\rho}_1 k_1 \cdot \hat{p}} e^{\frac{1}{2}(\tilde{\rho}_1 k_1^2 + \tilde{\rho}_2 k_2^2)} | p \rangle \\ &= \int \frac{d^d p}{(2\pi)^d} (2\pi)^d \delta^d(k_1 + k_2) w^{(\frac{p^2}{2} - \frac{d}{24})} e^{(\tilde{\rho}_1 k_1 + \tilde{\rho}_2 k_2) \cdot p - \frac{1}{2}(\tilde{\rho}_1 - \tilde{\rho}_2) k_1 \cdot k_2}, \quad (5.33) \end{aligned}$$

where in going to the last line we have used  $\hat{p}|p\rangle = p|p\rangle$  and  $\exp(ik\hat{x})|p\rangle = |p+k\rangle$ , and further  $\langle p|p+k_1+k_2\rangle = (2\pi)^d \delta^d(k_1+k_2)$  and  $k_1^2 = k_2^2 = -k_1 \cdot k_2$ . Taking account of the above remark for the P, NP and NO diagram cases, we here insert  $1 = \int d\alpha_F \delta(\alpha_F + 2p^+)$  and keep the  $\int d\alpha_F$  integration undone. Then

$$= \int d\alpha_F \delta(k_1 + k_2) w^{-d/24} \int d^d p \delta(\alpha_F + 2p^+) e^{\frac{1}{2}(\ln w)p^2 + (\tilde{\rho}_1 - \tilde{\rho}_2)k_1 \cdot p + \frac{1}{2}(\tilde{\rho}_2 - \tilde{\rho}_1)k_1 \cdot k_2}. \quad (5.34)$$

Completing the square in the exponent and making a shift of the integration variable  $p \rightarrow p - (\tilde{\rho}_1 - \tilde{\rho}_2)k_1 / \ln w$ , we find

$$\begin{aligned} &= \int d\alpha_F \delta(k_1 + k_2) w^{-d/24} \exp \left[ \left( \frac{(\tilde{\rho}_2 - \tilde{\rho}_1)^2}{2 \ln w} + \frac{\tilde{\rho}_2 - \tilde{\rho}_1}{2} \right) k_1 \cdot k_2 \right] \\ &\quad \times \int d^d p \exp \left( \frac{\ln w}{2} p^2 \right) \delta \left( \alpha_F + 2p^+ - \frac{\tilde{\rho}_1 - \tilde{\rho}_2}{\ln w} \alpha_1 \right). \quad (5.35) \end{aligned}$$

Using  $d^d p = d^{d-2} \mathbf{p} dp^+ dp^-$ ,  $p^2 = -2p^+ p^- + \mathbf{p}^2$  and  $\int dp^- e^{-(\ln w)p^+ p^-} = (-\frac{2\pi}{\ln w}) \delta(p^+)$ , the momentum integration in the second line yields

$$\left( \frac{-2\pi}{\ln w} \right)^{\frac{d}{2}} \delta \left( \alpha_F - \frac{\tilde{\rho}_1 - \tilde{\rho}_2}{\ln w} \alpha_1 \right). \quad (5.36)$$

If the  $\alpha_F$  dependence appeared only in this zero-mode sector, then the  $\alpha_F$  integration of the delta function would trivially give 1 and the expression (5.35) just reproduced the covariant case answer (5.29), as it should be. Therefore, the zero-mode trace in our case is given by

$$\text{Tr}_0[\cdots] = \int d\alpha_F \delta \left( \alpha_F - \frac{\tilde{\rho}_1 - \tilde{\rho}_2}{\ln w} \alpha_1 \right) \times [\text{covariant result Eq. (5.29)}]. \quad (5.37)$$

Secondly, note that the open string coordinate  $X(\rho_r)$  on the original  $\rho$  plane is usually an abbreviation for the real coordinate  $(X(\rho_r) + X(\bar{\rho}_r))/2$ , and is, therefore, mapped to the coordinate  $(X(\tilde{\rho}_r) + X(\bar{\tilde{\rho}}_r))/2$  on the final  $\tilde{\rho} = -2\pi i u$  plane, which coincides with  $X(\tilde{\rho}_r)$  if  $\tilde{\rho}_r$  lies on the real axis. This was actually the case in the P and NO diagram cases both for  $r = 1$  and 2. In the NP diagram case, however,  $\tilde{\rho}_2$  does not lie on the real axis, so that we should make a replacement

$$\begin{aligned} X^\mu(\tilde{\rho}_2) &\rightarrow \frac{1}{2} (X^\mu(\tilde{\rho}_2) + X^\mu(\bar{\tilde{\rho}}_2)) = \frac{1}{2} (X^\mu(\tilde{\rho}_2) + X^\mu(\tilde{\rho}_2 - 2\pi i)) \\ &= x^\mu - i\alpha_0^\mu(\tilde{\rho}_2 - \pi i) + i \sum_{n \neq 0} \frac{1}{n} \alpha_n^\mu e^{-n\tilde{\rho}_2}. \quad (5.38) \end{aligned}$$



This change amounts to making a replacement  $\tilde{\rho}_2 \rightarrow \tilde{\rho}_2 - \pi i$  only in the zero mode part in the above calculation, and hence the replacement of  $\psi(\rho, w)$  by

$$\begin{aligned}\psi(\rho, w) &\rightarrow \psi'(\rho, w) = \frac{1-\rho}{\sqrt{-\rho}} \exp\left(\frac{\ln^2(-\rho)}{2\ln w}\right) \prod_{n=1}^{\infty} \frac{(1-w^n\rho)(1-w^n/\rho)}{(1-w^n)^2} \\ &= \psi^T(-\rho, w),\end{aligned}\quad (5.39)$$

where

$$\psi^T(\rho, w) \equiv \frac{1+\rho}{\sqrt{\rho}} \exp\left(\frac{\ln^2 \rho}{2\ln w}\right) \prod_{n=1}^{\infty} \frac{(1+w^n\rho)(1+w^n/\rho)}{(1-w^n)^2}. \quad (5.40)$$

The  $\delta$  function factor in Eq. (5.37) is also modified by this shift  $\tilde{\rho}_2 \rightarrow \tilde{\rho}_2 - \pi i$ . But, thanks to this change,  $\tilde{\rho}_1 - \tilde{\rho}_2 = -2\pi i(Z_1 - Z_2)$  becomes  $4\pi i\tilde{\tau}x$  in coincidence with the P and NO cases. (Compare Eqs. (3.7) and (3.16).) Therefore, the  $\delta$  function factor in Eq. (5.37) can be rewritten uniformly in the three cases, P, NO and NP, into

$$\delta\left(\alpha_F - \frac{\tilde{\rho}_1 - \tilde{\rho}_2}{\ln w}\alpha_1\right) \rightarrow \delta\left(\frac{\tau_1 - \tau_2}{\ln w}\right) = (-\ln w)\delta(\tau_1 - \tau_2), \quad (5.41)$$

where use has been made of  $\ln w = 2\pi i\tilde{\tau} < 0$  and Eqs. (3.9), (3.13) and (3.18).

Finally, for the case of NO diagram where the period is  $\tilde{\tau} + 1/2$ , we should include the twist operator  $\Omega$ . Since  $\Omega\alpha_n\Omega^{-1} = (-)^n\alpha_n$ , the whole effect is simply to make a replacement  $w \rightarrow -w$  in the *non-zero mode* sector in Eq. (5.31); that is,

$$\begin{aligned}\psi(\rho, w) &\rightarrow \frac{1-\rho}{\sqrt{\rho}} \exp\left(\frac{\ln^2 \rho}{2\ln w}\right) \prod_{n=1}^{\infty} \frac{(1-(-w)^n\rho)(1-(-w)^n/\rho)}{(1-(-w)^n)^2} \equiv \psi^N(\rho, w), \\ f(w) &\rightarrow f(-w).\end{aligned}\quad (5.42)$$

Putting all these modifications together, and using a variable  $\rho_{12} \equiv e^{4\pi i\tilde{\tau}x}$  with which

$$e^{\tilde{\rho}_1 - \tilde{\rho}_2} = e^{-2\pi i(Z_1 - Z_2)} = \begin{cases} \rho_{12} & \text{for P and NO cases} \\ -\rho_{12} & \text{for NP case} \end{cases}, \quad (5.43)$$

we find the 2-point  $X$  correlation functions for P, NP and NO:

$$\left\langle e^{ik_2 \cdot X(Z_2)} e^{ik_1 \cdot X(Z_1)} \right\rangle = \int d\alpha_F (-\ln w) \delta(\tau_2 - \tau_1) \times \begin{cases} \mathcal{F} & \text{for P} \\ \mathcal{F}^T & \text{for NP} \\ \mathcal{F}^N & \text{for NO} \end{cases}, \quad (5.44)$$

where

$$\begin{aligned}\mathcal{F} &= (-2\pi i)^{-k_1 \cdot k_2} \delta^d(k_1 + k_2) \left(\frac{-2\pi}{\ln w}\right)^{\frac{d}{2}} \left[w^{\frac{1}{24}} f(w)\right]^{-d} [\psi(\rho_{12}, w)]^{k_1 \cdot k_2}, \\ \mathcal{F}^T &= (-2\pi i)^{-k_1 \cdot k_2} \delta^d(k_1 + k_2) \left(\frac{-2\pi}{\ln w}\right)^{\frac{d}{2}} \left[w^{\frac{1}{24}} f(w)\right]^{-d} [\psi^T(\rho_{12}, w)]^{k_1 \cdot k_2}, \\ \mathcal{F}^N &= (-2\pi i)^{-k_1 \cdot k_2} \delta^d(k_1 + k_2) \left(\frac{-2\pi}{\ln w}\right)^{\frac{d}{2}} \left[w^{\frac{1}{24}} f(-w)\right]^{-d} [\psi^N(\rho_{12}, w)]^{k_1 \cdot k_2}.\end{aligned}\quad (5.45)$$

5.3.3.  $UU$ 

As explained in Eq. (5.3), the correlation function for  $UU$  case is given by

$$\left\langle e^{ik_2 \cdot X(Z_2)} e^{ik_1 \cdot X(Z_1)} \right\rangle_\tau = (-2\pi i\tau)^{\frac{k_1^2}{2} + \frac{k_2^2}{2}} \text{Tr}' \left[ q^{2(L_0^X - \frac{d}{24})} : e^{ik_2 \cdot X(\tilde{\rho}_2^h)} :: e^{ik_1 \cdot X(\tilde{\rho}_1^h)} : \right] \quad (5.46)$$

where  $\tilde{\rho}_r^h = -2\pi i\tau Z_r$  and the zero-mode part trace is an expectation value:

$$\text{Tr}_0[\cdots] = \langle -k_1/2 | \cdots | -k_1/2 \rangle. \quad (5.47)$$

This zero-mode part ‘trace’ is immediately found by the help of Eq. (5.33) to give

$$\text{Tr}_0[\cdots] = (2\pi)^d \delta^d(k_1 + k_2) (q^2)^{-\frac{d}{24}} (q^{-\frac{1}{4}})^{k_1 \cdot k_2}. \quad (5.48)$$

The trace over the non-zero modes is essentially the same as before and is given by Eq. (5.30) by replacements  $w \rightarrow q^2$  and  $\tilde{\rho}_r \rightarrow \tilde{\rho}_r^h$ : so we have

$$\begin{aligned} & \left\langle e^{ik_2 \cdot X(Z_2)} e^{ik_1 \cdot X(Z_1)} \right\rangle_\tau \\ &= (-2\pi i\tau)^{-k_1 \cdot k_2} (2\pi)^d \delta^d(k_1 + k_2) \left[ q^{\frac{1}{12}} f(q^2) \right]^{-d} \left[ \tilde{\psi}(e^{\tilde{\rho}_1^h - \tilde{\rho}_2^h}, q^2) \right]^{k_1 \cdot k_2}, \end{aligned} \quad (5.49)$$

where

$$\tilde{\psi}(e^{\tilde{\rho}_1^h - \tilde{\rho}_2^h}, w) = q^{-\frac{1}{4}} e^{\frac{1}{2}(\tilde{\rho}_1^h - \tilde{\rho}_2^h)} \exp\left(-\frac{(\tilde{\rho}_1^h - \tilde{\rho}_2^h)^2}{2 \ln q^2}\right) \psi(e^{\tilde{\rho}_1^h - \tilde{\rho}_2^h}, q^2). \quad (5.50)$$

Noting the relations  $q = e^{i\pi\tau}$  and

$$e^{\tilde{\rho}_1^h - \tilde{\rho}_2^h} = e^{-2\pi i\tau(Z_1 - Z_2)} = e^{-4\pi i x + \pi i\tau} = q z_{12}^{-1} \quad (z_{12} \equiv e^{4\pi i x} \equiv e^{2\pi i \nu_{12}}), \quad (5.51)$$

in this  $UU$  case, this function  $\tilde{\psi}$  can be rewritten as follows:

$$\begin{aligned} \tilde{\psi}(e^{\tilde{\rho}_1^h - \tilde{\rho}_2^h}, w) &= q^{-\frac{1}{4}} \left( q z_{12}^{-1} \right)^{\frac{1}{2}} e^{-\frac{1}{4\pi i\tau} (2\pi i \nu_{12} - \pi i\tau)^2} \psi(q z_{12}^{-1}, q^2) \\ &= e^{-\pi i \nu_{12}^2 / \tau} \psi(q z_{12}^{-1}, q^2) = e^{-\pi i \nu_{12}^2 / \tau} \psi(q z_{12}, q^2) \end{aligned} \quad (5.52)$$

where in the last step we have used the properties (A.7),  $\psi(q^2 z, q^2) = -\psi(z, q^2)$  and  $\psi(z^{-1}, q^2) = -\psi(z, q^2)$  of the  $\psi$  function, explained in Appendix.

The expression (5.49) with this  $\tilde{\psi}$  can be rewritten in terms of  $\rho$  and  $w$ . Using the relation (A.5),

$$e^{-\pi i \nu_{12}^2 / \tau} \psi(q z_{12}, q^2) = -i\tau \psi^T(\rho_{12}, w), \quad (5.53)$$

in the Appendix and the first relation in Eq. (5.20), we find

$$\begin{aligned} & \left\langle e^{ik_2 \cdot X(Z_2)} e^{ik_1 \cdot X(Z_1)} \right\rangle_{UU} \\ &= (-2\pi i\tau)^{-k_1 \cdot k_2} (2\pi)^d \delta^d(k_1 + k_2) \left[ w^{\frac{1}{24}} f(w) \right]^{-d} \left( \frac{-2\pi}{\ln w} \right)^{\frac{d}{2}} \left[ -i\tau \psi^T(\rho_{12}, w) \right]^{k_1 \cdot k_2} \\ &= (2\pi)^d (\tau)^{-k_1 \cdot k_2} (-i\tau)^{k_1 \cdot k_2} \mathcal{F}^T = (-i)^{k_1 \cdot k_2} (2\pi)^d \mathcal{F}^T, \end{aligned} \quad (5.54)$$

with  $\mathcal{F}^T$  defined before in Eq. (5.45).

5.3.4.  $V_\infty$ 

The correlation function for  $V_\infty$  case is also calculated similarly to the  $UU$  case. By the formula (5.9) for this case, the zero-mode part trace  $\text{Tr}_0[\dots]$  is the expectation value  $\langle 0 | \dots | 0 \rangle$  with zero-momentum state, which can be read from Eq. (5.33) to give

$$\text{Tr}[\dots] = (2\pi)^d \delta^d(k_1 + k_2) (q^{1/2})^{-\frac{d}{24}} e^{-\frac{1}{4}(\tilde{\rho}_1^h - \tilde{\rho}_2^h)k_1 \cdot k_2}, \quad (5.55)$$

with  $-\pi i \tau Z_r = \tilde{\rho}_r^h/2$  used. As in the ghost part calculation, comparison of the formulas (5.9) and (5.2) shows that the trace over the non-zero modes in this case can be obtained by making replacements  $w \rightarrow q^{1/2}$ ,  $u \rightarrow (\tau/2)u$  and  $(-2\pi i) \rightarrow (-\pi i \tau)$  in the above result for NO case: so we have

$$\begin{aligned} \left\langle e^{ik_2 \cdot X(Z_2)} e^{ik_1 \cdot X(Z_1)} \right\rangle_{UU, \frac{\tau}{4} + \frac{1}{2}} &= (-\pi i \tau)^{-k_1 \cdot k_2} (2\pi)^d \delta^d(k_1 + k_2) \\ &\times \left[ q^{\frac{1}{48}} f(-\sqrt{q}) \right]^{-d} \left[ \exp\left(-\frac{(\tilde{\rho}_1^h - \tilde{\rho}_2^h)^2}{8 \ln q^{1/2}}\right) \tilde{\psi}^N(e^{\frac{1}{2}(\tilde{\rho}_1^h - \tilde{\rho}_2^h)}, q^{1/2}) \right]^{k_1 \cdot k_2}. \end{aligned} \quad (5.56)$$

Note that  $Z_1 - Z_2 = -2\tilde{\tau}x = \nu_{12}/\tau$  in this  $V_\infty$  case, so that

$$e^{\frac{1}{2}(\tilde{\rho}_1^h - \tilde{\rho}_2^h)} = e^{-\pi i \tau (Z_1 - Z_2)} = z_{12}^{-1/2}, \quad \exp\left(-\frac{(\tilde{\rho}_1^h - \tilde{\rho}_2^h)^2}{8 \ln q^{1/2}}\right) = e^{-\pi i \nu_{12}^2/\tau}. \quad (5.57)$$

We see that the quantity inside of  $[\dots]^{k_1 \cdot k_2}$  in Eq. (5.56) just equals  $(\tau/2)\psi^N(\rho_{12}, w)$  by the identity (A.6). Then using also the first relation in Eq. (5.23), we find

$$\begin{aligned} \left\langle e^{ik_2 \cdot X(Z_2)} e^{ik_1 \cdot X(Z_1)} \right\rangle_{UU, \frac{\tau}{4} + \frac{1}{2}} &= (-\pi i \tau)^{-k_1 \cdot k_2} (2\pi)^d \delta^d(k_1 + k_2) \\ &\times \left[ w^{\frac{1}{24}} f(-w) \right]^{-d} \left( \frac{-\pi}{\ln w} \right)^{\frac{d}{2}} \left[ \frac{\tau}{2} \psi^N(e^{\frac{1}{2}(\tilde{\rho}_1^h - \tilde{\rho}_2^h)}, q^{1/2}) \right]^{k_1 \cdot k_2} = \frac{(2\pi)^d}{2^{d/2}} \mathcal{F}^N. \end{aligned} \quad (5.58)$$

Incidentally, this relation together with Eq. (5.24) confirms the relation (5.10) announced before.

## §6. Explicit evaluation of tachyon amplitude

### 6.1. Amplitudes for $P$ , $NP$ , $NO$

Let us now evaluate the amplitudes (2.7) for  $P$ ,  $NP$  and  $NO$  explicitly. First the ghost part of the CFT correlation function in Eq. (2.8) is evaluated by mapping the integration contours on the  $\rho$  plane for the antighost factors  $b_{\tau_r}$  to those on the torus  $u$  plane:

$$\begin{aligned} &\langle b_{\tau_1} b_{\tau_2} c(Z_2) c(Z_1) \rangle_J \\ &= \int_{C_1} \frac{du_1}{2\pi i} \left( \frac{du_1}{d\rho} \right) \int_{C_2} \frac{du_2}{2\pi i} \left( \frac{du_2}{d\rho} \right) \langle b(u_1) b(u_2) c(Z_2) c(Z_1) \rangle_J \\ &= \mathcal{G}^J \int_{C_1} \frac{du_1}{2\pi i} \int_{C_2} \frac{du_2}{2\pi i} \left( \frac{du_1}{d\rho} \right) \left( \frac{du_2}{d\rho} \right) \left\{ \frac{d\rho}{du_1} - \frac{d\rho}{du_2} \right\} \\ &= \mathcal{G}^J \left( \int_{C_1} \frac{du_1}{2\pi i} \int_{C_2} \frac{du_2}{2\pi i} \frac{du_2}{d\rho} - \int_{C_2} \frac{du_2}{2\pi i} \int_{C_1} \frac{du_1}{2\pi i} \frac{du_1}{d\rho} \right) \end{aligned} \quad (6.1)$$

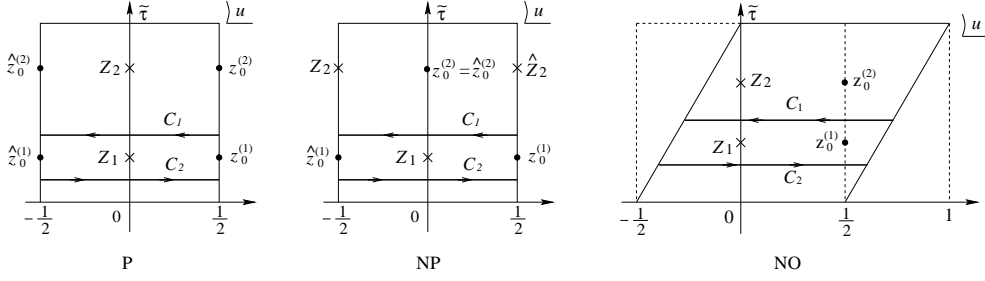


Fig. 10. The contours  $C_1$  and  $C_2$  giving antighost factors for P, NP and NO cases.

where we have used the results (5.16) and (5.18) for the ghost correlation functions and  $\mathcal{G}^J$  denotes

$$\mathcal{G}^J = \begin{cases} \mathcal{G} \equiv \frac{2\pi i}{\alpha_1} \left[ w^{\frac{1}{24}} f(w) \right]^2 & \text{for P, NP } (J = \tilde{\tau}) \\ \mathcal{G}^N \equiv \frac{2\pi i}{\alpha_1} \left[ w^{\frac{1}{24}} f(-w) \right]^2 & \text{for NO } (J = \tilde{\tau} + \frac{1}{2}) \end{cases}. \quad (6.2)$$

The contours  $C_1$  and  $C_2$  on the  $u$  plane are depicted in Fig. 10. Noting that  $du_2/d\rho$  is independent of  $u_1$  and vice versa, and  $\int_{C_r} du_r = \mp 1$  for  $r = 1$  and  $2$ , respectively, we can evaluate the contour integrations in Eq. (6.1) as follows:

$$\frac{-1}{2\pi i} \int_{C_2} \frac{du}{2\pi i} \frac{du}{d\rho} - \frac{1}{2\pi i} \int_{C_1} \frac{du}{2\pi i} \frac{du}{d\rho} = \frac{-1}{2\pi i} \int_{C_1+C_2} \frac{du}{2\pi i} \frac{du}{d\rho} = \frac{-1}{2\pi i} \oint_{z_0^{(1)}} \frac{du}{2\pi i} \frac{du}{d\rho}. \quad (6.3)$$

Noting that the integrand  $du/d\rho$  has a pole at  $u = z_0^{(1)}$  and the residue there

$$\text{Res}_{z_0^{(1)}} \left( \frac{du}{d\rho} \right) = \frac{1}{\alpha_1} \left[ g'_1(z_0^{(1)} - Z_1) - g'_1(z_0^{(1)} - Z_2) \right]^{-1} \equiv R, \quad (6.4)$$

we find

$$\langle b_{\tau_1} b_{\tau_2} c(Z_2) c(Z_1) \rangle_J = -\frac{R}{2\pi i} \mathcal{G}^J. \quad (6.5)$$

Next we rewrite the remaining  $X$  part and integrals  $d\tau_1 d\tau_2$  in Eq. (2.7) into

$$\begin{aligned} \int d\tau_1 d\tau_2 \left\langle e^{ik_2 \cdot X(Z_2)} e^{ik_1 \cdot X(Z_1)} \right\rangle_J &= \int d\tau_1 d\tau_2 d\alpha_F (-\ln w) \delta(\tau_2 - \tau_1) \mathcal{F}^J \\ &= \int d\tilde{\tau} dx \frac{i}{\pi} \alpha_1 R^{-1} (-\ln w) \mathcal{F}^J, \end{aligned} \quad (6.6)$$

where we have used the results (5.44) for the 2-point  $X$  correlation functions, the Jacobian (4.11) for  $(\tau_1, \alpha_F) \rightarrow (\tau, x)$  and the definition (6.4) of  $R$ .

Putting Eqs. (6.5) and (6.6) together, the amplitudes (2.7) for P, NO and NP are finally obtained as

$$\begin{pmatrix} \mathcal{A}_P \\ \mathcal{A}_{NP} \\ \mathcal{A}_{NO} \end{pmatrix} = -i \frac{\alpha_1}{(2\pi)^2} g^2 \int d\tilde{\tau} dx (-\ln w) \begin{pmatrix} n \mathcal{G} \mathcal{F} \\ \mathcal{G} \mathcal{F}^T \\ \mathcal{G}^N \mathcal{F}^N \end{pmatrix} / [(2\pi)^d \delta^d(k_1 + k_2)]$$

$$= -ig^2 \int d\left(\frac{\tilde{\tau}}{i}\right) dx \begin{pmatrix} n \left[ w^{\frac{1}{24}} f(w) (-2\pi \ln w)^{\frac{1}{2}} \right]^{-(d-2)} [\psi(\rho_{12}, w)]^{-2} \\ \left[ w^{\frac{1}{24}} f(w) (-2\pi \ln w)^{\frac{1}{2}} \right]^{-(d-2)} [\psi^T(\rho_{12}, w)]^{-2} \\ \left[ w^{\frac{1}{24}} f(-w) (-2\pi \ln w)^{\frac{1}{2}} \right]^{-(d-2)} [\psi^N(\rho_{12}, w)]^{-2} \end{pmatrix}. \quad (6.7)$$

In going to the last expressions, the explicit forms (5.45) for  $\mathcal{F}$ 's and Eqs. (5.19) and (5.18) for  $\mathcal{G}$ 's, are used together with the on-shell condition  $k_1 \cdot k_2 = -2$  and relations  $w = e^{2\pi i \tilde{\tau}}$ ,  $\rho_{12} = e^{4\pi i \tilde{\tau} x}$ .

### 6.2. Full nonplanar amplitude and $UU$ diagram

The nonplanar amplitude  $\mathcal{A}_{\text{NP}}$  in Eq. (6.7) gives a correct nonplanar on-shell tachyon amplitude<sup>12)</sup> if it covers the full integration region  $0 \leq \tilde{\tau}/i < \infty$  and  $0 \leq 2x(= \nu) \leq 1$ . However, the diagram in Fig. 7 does not cover the full region. The integration over  $x$  is all right since Eq. (3.18) with  $\tau_1 - \tau_2 = 0$  implies  $2x = \alpha_F/\alpha_1$  which indeed runs over  $0 \leq 2x \leq 1$  as  $\alpha_F$  runs from 0 to  $\alpha_1$ . But Eq. (3.19) implies that, as  $\tau_1$  runs from 0 to  $\infty$ ,  $\tilde{\tau}/i$  runs from a certain value  $\tilde{\tau}_0(x)/i (> 0)$  to  $\infty$ , where  $\tilde{\tau}_0(x)$  is the root for  $\tilde{\tau}$  of the Eq. (3.19) with  $\tau_1 = 0$ . So it is necessary to cover the missing region  $0 \leq \tilde{\tau}/i \leq \tilde{\tau}_0(x)/i$ .

As was announced already in §2, this missing region is covered by the  $UU$  diagram contribution (2.10), which we now evaluate explicitly.

The ghost part of the CFT correlation function (2.13) is calculated in quite the same way as in Eq. (6.1) by using Eq. (5.21) together with (5.16):

$$\begin{aligned} & \langle b_0 \bar{b}_0 c(Z_2) c(Z_1) \rangle_\tau \\ &= \int_{C_1} \frac{du_1}{2\pi i} \left( \frac{du_1}{d\rho} \right) \int_{C_2} \frac{du_2}{2\pi i} \left( \frac{du_2}{d\rho} \right) \langle b(u_1) b(u_2) c(Z_2) c(Z_1) \rangle_\tau \\ &= i\mathcal{G} \left( \int_{C_1} \frac{du_1}{2\pi i} \int_{C_2} \frac{du_2}{2\pi i} \frac{du_2}{d\rho} - \int_{C_2} \frac{du_2}{2\pi i} \int_{C_1} \frac{du_1}{2\pi i} \frac{du_1}{d\rho} \right). \end{aligned} \quad (6.8)$$

The contours  $C_1$  and  $C_2$  in this case are drawn in Fig. 11. Note that  $\int_{C_r} du_r 1 = \pm \tilde{\tau}$  for  $r = 1, 2$  instead of  $\mp 1$  in the previous case. Evaluating the remaining integration by the pole residue as done in Eq. (6.3), we obtain

$$\langle b_0 \bar{b}_0 c(Z_2) c(Z_1) \rangle_\tau = \frac{\tilde{\tau}}{2\pi} R \mathcal{G}. \quad (6.9)$$

The  $X$ -part of the correlation function was obtained in the Eq. (5.54) above, and the Jacobian for the change of variables  $(\tau_1, \sigma_1) \rightarrow (\tilde{\tau}, x)$  was given in Eq. (4.17), which reads  $d\tau_1 d\sigma_1 = i\alpha_1 R^{-1} d\tilde{\tau} dx$  by using  $R$  defined in Eq. (6.4). Putting these altogether, the  $UU$  amplitude (2.10) turns out to be

$$\mathcal{A}_{UU} = i\alpha_1 (-i)^{k_1 \cdot k_2} (2\pi)^{d-2} x_u^2 g^2 \int d\tilde{\tau} dx \tilde{\tau} \mathcal{G} \mathcal{F}^T / [(2\pi)^d \delta^d(k_1 + k_2)]$$

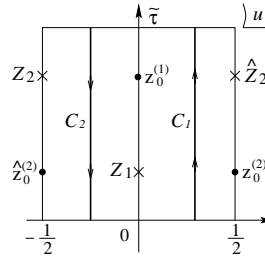


Fig. 11. The contours  $C_1$  and  $C_2$  for  $UU$  case.

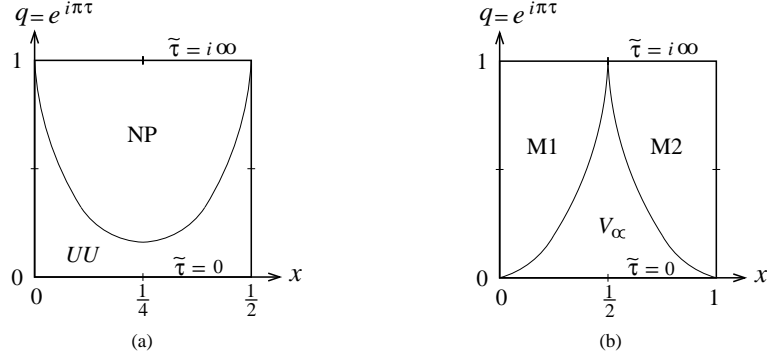


Fig. 12. A schematic view for the moduli regions covered by individual diagrams for the full (a) nonplanar and (b) nonorientable amplitudes.

$$= \frac{x_u^2}{(2\pi)^{1-d}} g^2 \int d\left(\frac{\tilde{\tau}}{i}\right) dx \left[ w^{\frac{1}{24}} f(w) (-2\pi \ln w)^{\frac{1}{2}} \right]^{-(d-2)} \left[ \psi^T(\rho_{12}, w) \right]^{-2}, \quad (6.10)$$

the same form as the above  $\mathcal{A}_{\text{NP}}$  in Eq. (6.7). So if the coefficients are the same with *opposite* sign, i.e.,

$$- \frac{x_u^2}{(2\pi)^{1-d}} g^2 = -ig^2 \quad \rightarrow \quad x_u^2 = i(2\pi)^{1-d} = \frac{i}{(2\pi)^{25}}, \quad (6.11)$$

then the full nonplanar amplitude is reproduced in this SFT. The reason of opposite sign is as follows. Originally, the variable  $\sigma_1$  runs from 0 to  $2\pi\alpha_1$  and  $\tau_1$  from 0 to  $\infty$ , which are mapped into the present variables  $x$  and  $\tilde{\tau}$  by the relations (3.30) and (3.31). From those relation we find the integration region correspondence

$$\int_0^{2\pi\alpha_1} d\sigma_1 \int_0^\infty d\tau_1 \leftrightarrow \int_0^{1/2} dx \int_{\tilde{\tau}_0(x)/i}^0 d\left(\frac{\tilde{\tau}}{i}\right) = - \int_0^{1/2} dx \int_0^{\tilde{\tau}_0(x)/i} d\left(\frac{\tilde{\tau}}{i}\right). \quad (6.12)$$

Namely a minus sign appears since the increasing direction of  $\tau_1$  is opposite to that of  $\tilde{\tau}/i$ , contrary to the previous NP case. This could have been inferred from the diagrams in Fig. 2, and indeed the relations (3.31) and (3.19) between  $\tau_1$  and  $\tilde{\tau}$  for UU and NP cases, respectively, have just opposite signs. Thus, with the coupling strength  $x_u^2$  in Eq. (6.11), we obtain the correct nonplanar amplitude  $\mathcal{A}_{\text{NP}}$  in Eq. (6.7) with the full integration region  $\int_0^\infty d(\tilde{\tau}/i) \int_0^{1/2} dx$ . In Fig. 12 (a), we present a schematic view to show how the two diagrams NP and UU cover the full moduli region  $0 \leq \tilde{\tau}/i < \infty$ ,  $0 \leq x \leq 1/2$ .

### 6.3. Full nonorientable amplitude and $V_\alpha$ diagram

In the same way, the amplitude  $\mathcal{A}_{\text{NO}}$  in Eq. (6.7) to which contribute the two nonorientable diagrams M1 and M2, does not yet cover the full region of the moduli,  $0 \leq \tilde{\tau}/i < \infty$ ,  $0 \leq x \leq 1$ . As explained in §2, the contributions of M1 and M2 diagrams have a gap in the moduli space and the  $V_\alpha$  diagram just gives the contribution filling the gap.

The ghost part of the CFT correlation function in the  $V_\alpha$  amplitude (2.14) is calculated in a similar way to the preceding two cases (6.1) and (6.8). Noting that

the anti-ghost factors  $b_{\sigma_i}$  ( $i = 1, 2$ ) in this case are defined on the  $\rho$  plane as

$$b_{\sigma_i} \equiv \frac{d\rho_0^{(i)}}{d\sigma_i} \int_{C_i} \frac{d\rho}{2\pi i} b(\rho) = i \int_{C_i} \frac{d\rho}{2\pi i} b(\rho), \quad (6.13)$$

and mapping them into the torus  $u$  plane, we evaluate the ghost part as follows:

$$\begin{aligned} & \langle b_{\sigma_1} b_{\sigma_2} c(Z_2) c(Z_1) \rangle_{\frac{\tau}{4} + \frac{1}{2}} \\ &= i^2 \int_{C_1} \frac{du_1}{2\pi i} \left( \frac{du_1}{d\rho} \right) \int_{C_2} \frac{du_2}{2\pi i} \left( \frac{du_2}{d\rho} \right) \langle b(u_1) b(u_2) c(Z_2) c(Z_1) \rangle_{\frac{\tau}{4} + \frac{1}{2}} \\ &= -i\mathcal{G}^N \left( \int_{C_1} \frac{du_1}{2\pi i} \int_{C_2} \frac{du_2}{2\pi i} \frac{du_2}{d\rho} - \int_{C_2} \frac{du_2}{2\pi i} \int_{C_1} \frac{du_1}{2\pi i} \frac{du_1}{d\rho} \right) \\ &= -i\mathcal{G}^N \frac{2\tilde{\tau}}{2\pi i} \int_{C_1 - C_2} \frac{du}{2\pi i} \frac{du}{d\rho} = -i\mathcal{G}^N \frac{2\tilde{\tau}}{2\pi i} \left( \oint_{z_0^{(1)}} - \oint_{z_0^{(2)}} \right) \frac{du}{2\pi i} \frac{du}{d\rho} \\ &= -\frac{4\tilde{\tau}}{2\pi} R \mathcal{G}^N, \end{aligned} \quad (6.14)$$

where the contours  $C_1$  and  $C_2$  on the  $u$  plane are those shown in Fig. 13, and we have used Eqs. (5.24) and (5.18),  $\int_{C_r} du_r 1 = -2\tilde{\tau}$  for both  $r = 1$  and  $2$  and the fact that the residues of  $du/d\rho$  at the poles  $z_0^{(1)}$  and  $z_0^{(2)}$  are  $\pm R$ , respectively.

The  $X$ -part of the correlation function was given in Eq. (5.58), and the Jacobian for the change of variables  $(\sigma_1, \sigma_2) \rightarrow (\tilde{\tau}, x)$  was calculated in Eq. (4.15), which is written as  $d\sigma_1 d\sigma_2 = -(\alpha_1/2) R^{-1} d\tilde{\tau} dx$  by using the residue  $R$ . Putting these altogether, the  $V_\infty$  amplitude (2.14) is found to be

$$\begin{aligned} \mathcal{A}_{V_\infty} &= \frac{(2\pi)^d}{2^{d/2}} \frac{\alpha_1}{\pi} x_\infty g^2 \\ &\times \int d\tilde{\tau} dx \tilde{\tau} \mathcal{G}^N \mathcal{F}^N / [(2\pi)^d \delta^d(k_1 + k_2)] \\ &= \frac{(2\pi)^d}{2^{d/2}} 2i x_\infty g^2 \int d\left(\frac{\tilde{\tau}}{i}\right) dx \left[ w^{\frac{1}{24}} f(-w) (-2\pi \ln w)^{\frac{1}{2}} \right]^{-(d-2)} \left[ \psi^N(\rho_{12}, w) \right]^{-2}. \end{aligned} \quad (6.15)$$

This again correctly gives the same form as the nonorientable amplitude  $\mathcal{A}_{\text{NO}}$  in Eq. (6.7). In this case the moduli integration directions are the same as is seen shortly, therefore, the full nonorientable amplitude is reproduced in our SFT if their coefficients are the same with the same sign:

$$\frac{(2\pi)^d}{2^{d/2}} 2i x_\infty g^2 = -ig^2 \quad \rightarrow \quad x_\infty = -\frac{2^{d/2}}{2(2\pi)^d}. \quad (6.16)$$

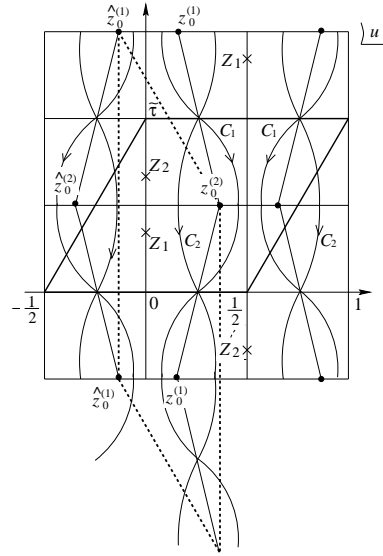


Fig. 13. The contours  $C_1$  and  $C_2$  for  $V_\infty$  case.

Originally the  $V_\infty$  vertex has a moduli integration  $\int_{0 \leq \sigma_1 \leq \sigma_2 \leq \pi\alpha_1} d\sigma_1 d\sigma_2$  which corresponds to  $\int_0^{\pi\alpha_1} d\sigma_+ \int_0^{\sigma_+} d\sigma_-$  (for M1 diagram) plus  $\int_{\pi\alpha_1}^{2\pi\alpha_1} d\sigma_+ \int_0^{2\pi\alpha_1 - \sigma_+} d\sigma_-$  (for M2 diagram), in terms of  $\sigma_\pm \equiv \sigma_2 \pm \sigma_1$ . Inspection of Eqs. (3·25) and (3·26) shows that this integration region corresponds just to  $\int_0^1 dx \int_0^{\tilde{\tau}_0(x)/i} d(\tilde{\tau}/i)$ , where the boundary value  $\tilde{\tau}_0(x)$  is given by the root for  $\tilde{\tau}$  of Eq. (3·26) with  $\sigma_- = 2\pi\alpha_1 x$  for  $x \leq 1/2$  and  $\sigma_- = 2\pi\alpha_1(1-x)$  for  $x \geq 1/2$ . More explicitly, from Eq. (3·26), we see that  $y = 0$  corresponds to  $\sigma_- = 2\pi\alpha_1 x$  and  $y = 1/2$  to  $\sigma_- = 2\pi\alpha_1(1-x)$ , so that the boundary value  $\tilde{\tau}_0(x)$  is determined by Eq. (3·27) with  $y = 0$  and  $1/2$ :

$$-2\pi i x = \begin{cases} g_2(\tilde{\tau}x|\tilde{\tau} + 1/2)|_{\tilde{\tau}=\tilde{\tau}_0(x)} & \text{for } x \leq 1/2 \\ g_2(\tilde{\tau}x + 1/2|\tilde{\tau} + 1/2)|_{\tilde{\tau}=\tilde{\tau}_0(x)} & \text{for } x \geq 1/2 \end{cases} \quad (6\cdot17)$$

The former equation for  $x \leq 1/2$  just coincides with Eq. (3·15) with  $y = 0$  for nonorientable M1 case, where  $y = 0$  for M1 case corresponds to the  $\tau_1 = 0$  boundary as is seen in Eq. (3·14). Thus M1 diagram covers the moduli region  $\int_0^{1/2} dx \int_{\tilde{\tau}_0(x)/i}^\infty d(\tilde{\tau}/i)$ , and, similarly, the M2 diagram covers the region  $\int_{1/2}^1 dx \int_{\tilde{\tau}_0(x)/i}^\infty d(\tilde{\tau}/i)$  (although we have not written the mapping explicitly for the latter case). In Fig. 12 (b), it is shown how the full moduli region  $0 \leq \tilde{\tau}/i < \infty$ ,  $0 \leq x \leq 1$  is covered by these three diagrams.

#### 6.4. Singularities of planar and $V_\infty$ amplitudes

The planar amplitude  $\mathcal{A}_P$  in Eq. (6·7) and the  $V_\infty$  amplitude (6·15) both have a singularity coming from the configuration drawn in Fig. 4. These singularities should cancel each other between these two amplitudes in order for the theory to be consistent.

To analyze the singularity, we first rewrite the planar amplitude  $\mathcal{A}_P$  in Eq. (6·7) in terms of the variables  $(q, \nu)$  in place of  $(w, x)$ :

$$\begin{cases} q = e^{i\pi\tau} = e^{-i\pi/\tilde{\tau}} \\ \nu_{12} = 2x \end{cases} \leftrightarrow \begin{cases} w = e^{2\pi i\tilde{\tau}} \\ \rho_{12} = e^{4\pi i\tilde{\tau}x} = e^{2\pi i\nu_{12}} \end{cases} \quad (6\cdot18)$$

Noting that the integrand is rewritten as

$$\begin{aligned} \psi(\rho_{12}, w) &= \left( \frac{-2\pi}{\ln q} \right) \sin \pi \nu_{12} \prod \frac{1 - 2q^{2n} \cos 2\pi \nu_{12} + q^{4n}}{(1 - q^{2n})^2} \equiv \left( \frac{-2\pi}{\ln q} \right) F(\nu_{12}, q^2), \\ \left[ w^{\frac{1}{24}} f(w) (-2\pi \ln w)^{\frac{1}{2}} \right] &= (2\pi) \left[ q^{\frac{1}{12}} f(q^2) \right], \end{aligned} \quad (6\cdot19)$$

and also using

$$dx = \frac{1}{2} d\nu_{12}, \quad d(\tilde{\tau}/i) = \frac{d\tau}{i\tau^2} = \frac{\pi}{(\ln q)^2} \frac{dq}{q}, \quad (6\cdot20)$$

we find

$$\begin{aligned} \mathcal{A}_P &= -i n g^2 \int \frac{dq}{q} d\nu_{12} \frac{1}{2} \frac{\pi}{(\ln q)^2} (2\pi)^{-(d-2)} \left( \frac{-2\pi}{\ln q} \right)^{-2} \left[ q^{\frac{1}{12}} f(q^2) \right]^{-(d-2)} \left[ F(\nu_{12}, q^2) \right]^{-2} \\ &= -\frac{i n g^2}{(2\pi)^d} \frac{\pi}{2} \int \frac{dq}{q} d\nu_{12} q^{-\frac{d-2}{12}} \left[ f(q^2) \right]^{-(d-2)} \left[ F(\nu_{12}, q^2) \right]^{-2} \\ &= -\frac{i n g^2}{(2\pi)^{26}} \frac{\pi}{2} \int_0^1 \frac{dq}{q^3} \int_0^1 d\nu_{12} \left[ f(q^2) \right]^{-24} \left[ F(\nu_{12}, q^2) \right]^{-2} \quad (\text{at } d = 26). \end{aligned} \quad (6\cdot21)$$



In the final equation we have made the integration region explicit.

Next we rewrite the  $V_\infty$  amplitude (6.15), or more precisely the full nonorientable amplitude  $\mathcal{A}_{V_\infty} + \mathcal{A}_{\text{NO}} = \mathcal{A}_{V_\infty + \text{NO}}$ , into a similar form using the same variables  $(q, \nu)$ . The integrand is rewritten as

$$\begin{aligned} \psi^N(\rho_{12}, w) &= \left( \frac{-4\pi}{\ln q} \right) \sin \frac{\pi \nu_{12}}{2} \prod \frac{1 - 2(-\sqrt{q})^n \cos \pi \nu_{12} + q^n}{(1 - (-\sqrt{q})^n)^2} \\ &= \left( \frac{-4\pi}{\ln q} \right) F\left(\frac{\nu_{12}}{2}, -\sqrt{q}\right), \\ \left[ w^{\frac{1}{24}} f(-w) (-2\pi \ln w)^{\frac{1}{2}} \right] &= 2^{-\frac{1}{2}} (2\pi) \left[ q^{\frac{1}{48}} f(-\sqrt{q}) \right], \end{aligned} \quad (6.22)$$

using the same function  $F$  as defined in Eq. (6.19). Also using the coupling relation (6.16), we obtain

$$\begin{aligned} \mathcal{A}_{V_\infty + \text{NO}} &= -\frac{ig^2}{(2\pi)^d} 2^{\frac{d}{2}-4} \pi \int \frac{dq}{q} d\nu_{12} q^{-\frac{d-2}{48}} [f(-\sqrt{q})]^{-(d-2)} \left[ F\left(\frac{\nu_{12}}{2}, -\sqrt{q}\right) \right]^{-2} \\ &= -\frac{ig^2}{(2\pi)^{26}} 2^9 \pi \int \frac{dq}{q^{\frac{3}{2}}} d\nu_{12} [f(-\sqrt{q})]^{-24} \left[ F\left(\frac{\nu_{12}}{2}, -\sqrt{q}\right) \right]^{-2} \end{aligned} \quad (6.23)$$

at  $d = 26$ . If we perform a further change of the variables,

$$\frac{\nu_{12}}{2} = \nu'_{12}, \quad \sqrt{q} = q'^2 \quad \rightarrow \quad d\nu_{12} = 2d\nu'_{12}, \quad dq = 4q'^3 dq', \quad (6.24)$$

the amplitude can be cast into almost the same form as  $\mathcal{A}_P$ :

$$\mathcal{A}_{V_\infty + \text{NO}} = -\frac{ig^2}{(2\pi)^{26}} 2^{12} \pi \int_0^1 \frac{dq'}{q'^3} \int_0^1 d\nu'_{12} [f(-q'^2)]^{-24} \left[ F(\nu'_{12}, -q'^2) \right]^{-2}, \quad (6.25)$$

where again the integration region has been made explicit. Note that  $\nu_{12} = 2x$  runs over the range  $[0, 2]$  in this full nonorientable amplitude so that  $\nu'_{12}$  runs over the same range  $[0, 1]$  as the previous  $\nu_{12}$  in the P case.

Now we can compare the two amplitudes (6.21) and (6.25). The singularities occur at  $q^2 = 0$ , around which the integrand function is expanded as

$$[f(q^2)]^{-24} [F(\nu, q^2)]^{-2} = \sin \pi \nu \left[ 1 + 4(\cos 2\pi \nu + 5)q^2 + O(q^4) \right]. \quad (6.26)$$

Since this is integrated with the measure  $dq/q^3$ , the first and the second terms of this expansion yield singularities corresponding to the (closed) tachyon and dilaton, respectively. Noting that the argument  $q^2$  is replaced by  $-q^2$  for the  $\mathcal{A}_{V_\infty + \text{NO}}$  case, the latter dilaton singularity can be cancelled between  $\mathcal{A}_P$  and  $\mathcal{A}_{V_\infty + \text{NO}}$  if

$$\frac{-ig^2}{(2\pi)^{26}} \frac{\pi}{2} + (-1) \frac{-ig^2}{(2\pi)^{26}} 2^{12} \pi = 0 \quad \Rightarrow \quad n = 2^{13}. \quad (6.27)$$

Namely, our gauge group  $SO(n)$  must be  $SO(2^{13})$ .<sup>18), 19), 20), 21)</sup>

At this point we recall the relation (1.6),  $x_\infty = nx_u^2 = -4\pi i x_\infty$ , derived in I. This demands, in particular, the equality  $nx_u^2 = -4\pi i x_\infty$ . But, here in the above, we have

determined all of  $n$ ,  $x_u^2$  and  $x_\infty$  by computing the loop amplitudes. Substituting the above results (6.11), (6.16) and (6.27), we see that this equality is actually satisfied. This gives a rather nontrivial consistency check for the present theory.

There remains, however, a stronger singularity due to tachyon contribution which under the condition (6.27) adds up between  $\mathcal{A}_P$  and  $\mathcal{A}_{V_\infty+NO}$ :

$$\begin{aligned} 2 \times \frac{\pi - i n g^2}{2 (2\pi)^{26}} \int_0^1 \frac{dq}{q^3} \int_0^1 d\nu \sin \pi \nu &= -\frac{n x_u^2 g^2}{2} \lim_{\varepsilon \rightarrow 0} \int_0^1 d\nu \sin \pi \nu \int_{\varepsilon(8\alpha_1 \sin \pi \nu)^{-1}}^1 \frac{dq}{q^3} \\ &= -\frac{n x_u^2 g^2}{2} \lim_{\varepsilon \rightarrow 0} \frac{32\alpha_1^2}{\varepsilon^2} \int_0^1 d\nu \sin^3 \pi \nu = -\frac{n x_u^2 g^2}{2} \lim_{\varepsilon \rightarrow 0} \frac{32\alpha_1^2}{\varepsilon^2} \frac{4}{3\pi}, \end{aligned} \quad (6.28)$$

where  $x_u^2 = i(2\pi)^{-25}$  is used and the singular endpoint of the  $q$  integration has been cut off by the time length  $\tau_1 \geq \varepsilon$  on the  $\rho$ -plane, which corresponds to the cutoff  $q \geq \varepsilon(8\alpha_1 \sin \pi \nu)^{-1}$  by the mapping relations (3.10) and (3.11). [For  $q \ll 1$ , we have  $y = 1/4 + O(q^2)$  from Eq. (3.11), and  $\tau_1/2\alpha_1 = 4q \sin \pi \nu$  from Eq. (3.10).] On the other hand, as in the case of closed tachyon amplitude considered in I, we still have another contribution to this amplitude, coming from the counterterm which was introduced as a ‘renormalization’ of the zero intercept. The counterterm is contained in  $\tilde{Q}_B^0 = Q_B^0 + \lambda_o g^2 \alpha^2 c_0$ , and so contributes to the open tachyon amplitude as

$$\begin{aligned} (2\pi)^d \delta^d(k_1 + k_2) \mathcal{A}_{\text{count}} &= -\langle R^0(1, 2) | \varphi^0(k_2) \rangle_2 \lambda_o g^2 \alpha_1^2 c_0^{(1)} | \varphi^0(k_1) \rangle_1 \\ \Rightarrow \quad \mathcal{A}_{\text{count}} &= -\lambda_o \alpha_1^2 g^2 = +\alpha_1^2 g^2 \lim_{\varepsilon \rightarrow 0} \frac{32 n x_u^2}{2\varepsilon^2}, \end{aligned} \quad (6.29)$$

where the value (1.5) for  $\lambda_o = \lambda_c/2$  has been substituted. Unfortunately, this contribution seems *not* to cancel the divergence in Eq. (6.28) since the coefficients differ by a factor  $4/3\pi$ . However, we should note that the problem is very subtle since they are divergent quantities; indeed, the value for  $\lambda_o = \lambda_c/2$  used in Eq. (6.29) was determined in I considering the cancellation of similar divergences in the case of closed string tachyon amplitude. So the identification of the cutoff parameters  $\varepsilon$  on the  $\rho$  plane in both terms may not be suitable since the present  $\rho$  plane of the open tachyon amplitude has boundaries while that of the previous closed tachyon amplitude does not. It is also unclear whether there is no other suitable cutoff procedure with which exact cancellation can be realized. At the moment, unfortunately, we cannot show that the divergence due to the presence of tachyon is cancelled by the renormalization of the ‘zero intercept’ term  $\lambda_o g^2 \alpha^2 c_0$ , although there is still a chance of cancellation since Eqs. (6.28) and (6.29) have *opposite* signs in any case.

## §7. Conclusion and discussions

We have shown that the (open) tachyon one-loop 2-point amplitudes are correctly reproduced in our SFT by choosing the coupling constants suitably. All the coupling constants of the seven interaction vertices have now been determined. Some relations among the coupling constants which are found in the previous two papers and this paper, turn out to be mutually consistent.

Nevertheless the presence of tachyon is a problem in our SFT, as is always the case in bosonic string theories. The (closed) tachyon vanishing into vacuum causes divergences in various amplitudes. As we have seen at the end of the last section, it is not clear that even the on-shell amplitudes can be made finite at loop levels by the ‘renormalization’ of the ‘zero-intercept term’ proportional to  $\alpha^2$  in  $\tilde{Q}_B$ . Moreover, off the mass-shell, the amplitudes even at the tree level *cannot* be made finite by such simple counterterms. Indeed, in the closed tachyon 2-point amplitude considered in I, the cancellation condition of the divergences between the disk (D) and real projective plane (RP) amplitudes becomes different off the mass-shell, where the conformal factors  $(\prod_r dZ_r/dw_r)^{k^2/8-1}$  become contributing and the imbalance of them between the D and RP amplitude cases yield the terms proportional to  $k^2 - 8$  and  $(k^2 - 8)^2$  at  $O(q)$  and  $O(q^2)$ . Since the tachyon singularity is as singular as  $\int dq/q^3$ , even such ‘small’ differences of  $O(q)$  and  $O(q^2)$  lead to divergences, proportional to operators  $L + \bar{L}$  and  $(L + \bar{L})^2$ .

In our computations of one-loop tachyon 2-point amplitudes in this paper, we had the delta function factor  $\delta(\tau_1 - \tau_2)$ , with which factor the string diagrams such as in Fig. 1 reduced to the same diagrams as those appearing in the light-cone gauge SFT.<sup>22),14)</sup> So the discussions became almost the same as in the light-cone gauge SFT. For instance, the nonplanar diagram (a) in Fig. 2 did not cover the whole moduli region of the nonplanar one-loop amplitude and required the existence of the  $UU$  diagram (b) in Fig. 2, hence explaining the reason of existence of the open-closed transition vertex  $U$ .<sup>14)</sup> Actually, in the light-cone gauge SFT, the former nonplanar diagram (a) is anomalous from the viewpoint of Lorentz-invariance and the anomaly is cancelled by the diagram (b) at  $\tau = 0$ . This was shown by Saito and Tanii<sup>9),10)</sup> and Kikkawa and Sawada.<sup>11)</sup>

In the light-cone gauge SFT, there is a universal time (light-cone time) in which the interactions are local and the time lengths are the same along whichever the paths on the diagram they are measured. Namely, the diagrams in the light-cone gauge SFT are always stretched *tight*, and there appear no diagrams with propagators which are *slack* or propagating *backward* in the time. The presence of such universal time was essential in the proof of physical equivalence of the light-cone gauge SFT to the covariant Polyakov formulation (hence of the modular and Lorentz invariance of the light-cone gauge SFT).<sup>23)</sup>

The ultimate reason why the diagrams become tight in the light-cone gauge string (or particle) field theory resides in the fact that the vertices there have no dependence on  $P^-$ , the  $-$  components of momenta other than in momentum conservation  $\delta$  function: suppose, for instance, that two vertices are connected by two propagators 1 and 2 simultaneously, thus making a loop. The two propagators can be represented as

$$\frac{1}{p_r^2 + M^2} = \int_0^\infty dT_r e^{-(p_r^2 + M^2)T_r} = \int_0^\infty dT_r e^{[2p_r^+ p_r^- - (p_r^2 + M^2)]T_r}, \quad (7.1)$$

using proper times  $T_r$  for each string (or particle)  $r = 1, 2$  with  $M^2$  being squared mass (operator). The momenta  $p_r$  can be represented as  $p_1 = l$  and  $p_2 = k - l$  by using the loop momentum  $l$  and a certain external momentum  $k$ . Then, if the two vertices

have no dependence on the  $-$  components of momenta, i.e., are *independent* of  $l^-$  in this case, the  $l^-$  dependence appears only in the propagators and we can perform the  $l^-$  integration of the loop integral  $\int d^d l / (2\pi)^d$  as follows, writing  $2p_r^+ = \alpha_r$ :

$$\int \frac{dl^-}{2\pi} e^{\alpha_1 l^- T_1} e^{\alpha_2 (k^- - l^-) T_2} = e^{\alpha_2 k^- T_2} \delta(\alpha_1 T_1 - \alpha_2 T_2) = e^{k^- \tau_2} \delta(\tau_1 - \tau_2). \quad (7.2)$$

Namely, the equality of the light-cone times  $\tau_r = \alpha_r T_r$  resulted for  $r = 1$  and 2. The same thing happens for any more complicated diagrams and the diagrams become stretched tight.

In our  $\alpha = p^+$  HIKKO type SFT,<sup>7)</sup> on the other hand, the vertices *has* the dependence on  $P^-$  and, therefore, there generally appear ‘slack’ diagrams. As was explained in some detail in the Appendix B of Ref. 7), if all the external string states contain no excitations of  $\alpha_n^-$  modes, the  $P^-$  dependent part of the vertices plays no role and can be discarded, and then only ‘tight’ diagrams as in the light-cone gauge case can contribute to the process. This was actually the case in our computation of the tachyon amplitudes in this paper since the tachyon has no excitation of  $\alpha_n^\mu$  modes at all.

If we consider more general external states, however, all the slack diagrams, and even those with propagators propagating backward in the light-cone time, become contributing. This is the case, in particular, when we try to prove the BRS invariance of the effective action  $\Gamma[\Psi, \Phi]$  possessing general external string fields  $\Psi, \Phi$ . Therefore the BRS invariance proof at loop level would look rather different from the computations in the present paper. Consider, for instance, the one-loop effective action  $\Gamma_{1\text{-loop}}[\Psi]$  quadratic in open-string field  $\Psi$  in Eq. (2.1) which contains the planar diagram contribution

$$\Gamma_{1\text{-loop}}^{\text{planar}}[\Psi] = i \frac{g^2}{4} \int_0^\infty d\tau_1 d\tau_2 n \langle v_P(\tau_1, \tau_2) | b_{\tau_1} b_{\tau_2} | \Psi \rangle_2 | \Psi \rangle_1, \quad (7.3)$$

This term generally corresponds to slack planar diagram in Fig. 1 with  $\tau_1 \neq \tau_2$ . Now act the BRS operator on the two external fields  $\Psi_r$ . Then, as being a general property,<sup>6)</sup> BRS operator acts as an differential operator on the moduli parameters,  $\tau_1$  and  $\tau_2$  in this case, and obtain two surface terms with  $\int d\tau_1 \langle v_P(\tau_1, \tau_2=0) | b_{\tau_1}$  and  $\int d\tau_2 \langle v_P(\tau_1=0, \tau_2) | b_{\tau_2}$ . The former term, for instance, corresponds to the diagram in which the second propagator is collapsed. Which contribution does this term cancel with?

Generically, the loop-level action is BRS invariant if the (tree level) action  $S$  is. This should be the case also here. In fact, consider the tree diagrams drawn in Fig. 14 and recall that the BRS invariance was realized among those three diagrams;<sup>24), 14)</sup> the BRS transformation of the diagrams (a) and (c) leaves the surface terms of the moduli  $\tau$  and  $\tau'$  at  $\tau = 0$  and  $\tau' = 0$ , respectively. But the BRS transform of the diagram (b) with quartic interaction  $V_4^0$ , yields the surface terms of the moduli  $\sigma_0$  at  $\sigma_0 = 0$  and  $\pi |\alpha_4|$ . These are the same configurations as the above two surface terms of the diagrams (a) at  $\tau = 0$  and (c) at  $\tau' = 0$  and cancel them.

This cancellation mechanism should also work when these tree diagrams are lifted to loop diagrams. Indeed, if the strings 3 and 4 have the same length, i.e.,

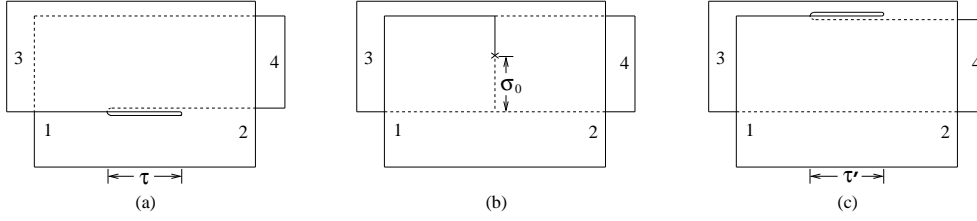


Fig. 14. A set of tree diagrams among which BRS invariance is satisfied.

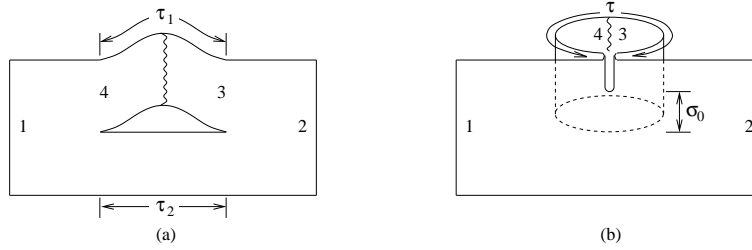


Fig. 15. Loop diagrams obtained from the tree diagrams (a) and (b) in Fig. 14 by contracting strings 3 and 4.

$\alpha_3 = |\alpha_4|$ , we can connect the strings 3 and 4 and make one-loop diagrams (a) and (b) drawn in Fig. 15. In this case of  $\alpha_3 = |\alpha_4|$ , the diagram (c) disappears. Note that the diagram (a) in Fig. 15 is nothing but the ‘slack’ planar diagram, and that the diagram at  $\tau_2 = 0$  is just the surface term which we have been discussing in the above. As is now clear from the above tree level arguments, it is cancelled by the diagram (b) in Fig. 15 at  $\sigma_0 = 0$  which is left as a surface term when the diagram (b) is BRS transformed. (A surface term at another endpoint  $\sigma_0 = \pi |\alpha_4|$  would probably not contribute since it gives a disconnected diagram.) The diagram (b) gives another surface term at  $\tau = 0$ , but it is as yet not clear whether it vanishes by itself or not.

Finally, we consider two tree diagrams in Fig. 16, the sum of which is clearly BRS invariant since the surface terms at  $\tau = 0$  from those two are the same and cancel. If strings 3 and 4 have the same length,  $\alpha_3 = |\alpha_4|$ , we can again connect the strings 3 and 4 and obtain one-loop diagrams (a) and (b) drawn in Fig. 17. The resultant diagram (a) is nothing but the nonplanar diagram, generally slack  $\tau_1 \neq \tau_2$ . For generic external states, both diagrams (a) and (b) contribute and their surface terms at  $\tau_2 = 0$  are the same and cancel with each other. So generically the BRS invariance holds with these two diagrams alone. However, if the external states  $\Psi_r$  contain no  $\alpha_n^-$  modes, then the delta function factor  $\delta(\tau_1 - \tau_2)$  appears and only the tight diagrams can contribute. This implies that the diagram (b) which contains backward propagation (i.e.,  $\tau_1 = \alpha_4 T_1 < 0$ ) does not contribute from the start, and thus the counterterm which can cancel the surface term at  $\tau_1 = \tau_2 = 0$  of diagram (a) becomes missing. This is an anomaly of the BRS invariance in our SFT. As demonstrated in the present paper, the desired counterterm is supplied by the  $UU$  diagram (b) in Fig. 2. We suspect that the BRS anomalies in our SFT occur this way only when the external states  $\Psi_r$  contain no  $\alpha_n^-$  modes. If so, then the relevant

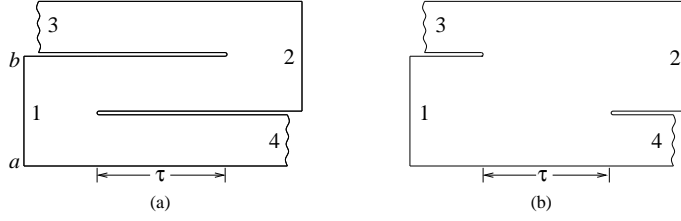


Fig. 16. Another set of tree diagrams satisfying BRS invariance.

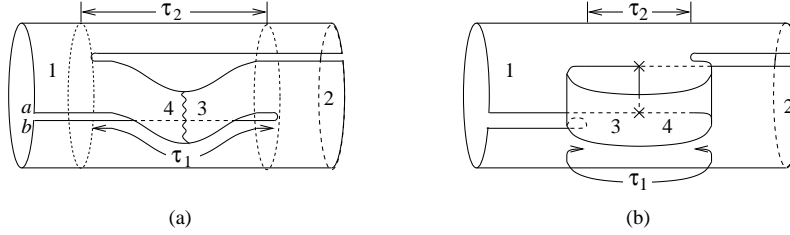


Fig. 17. Loop diagrams obtained from the tree diagrams (a) and (b) in Fig. 16 by contracting strings 3 and 4.

diagrams are always tight ones as in the light-cone gauge SFT and the anomalies for BRS and Lorentz invariance in both theories will come from the same type of diagrams.

### Acknowledgements

The authors would like to express their sincere thanks to H. Hata, H. Itoyama, M. Kato, K. Kikkawa, N. Ohta, M. Maeno, Y. Matsuo, S. Sawada, K. Suehiro, Y. Watabiki and T. Yoneya for valuable and helpful discussions. They also acknowledge hospitality at Summer Institute Kyoto '97 and '98. T. K. and T. T. are supported in part by the Grant-in-Aid for Scientific Research (#10640261) and the Grant-in-Aid (#6844), respectively, from the Ministry of Education, Science, Sports and Culture.

### Appendix A

—  $\psi(\rho, w)$  and  $\psi(z, q^2)$  —

In the text, we have used the same variables as defined in GSW:<sup>12)</sup>

$$\begin{cases} \rho = e^{2\pi i \tilde{\tau} \nu} \\ w = e^{2\pi i \tilde{\tau}} \end{cases}, \quad \begin{cases} z = e^{2\pi i \nu} \\ q^2 = e^{2\pi i \tau} \end{cases}, \quad (\text{A.1})$$

with  $\tau = -1/\tilde{\tau}$ . Then, clearly,  $(z, q^2)$  corresponds to  $(\nu, \tau)$  by the same relation as  $(\rho, w)$  to  $(\tilde{\nu} \equiv \tilde{\tau} \nu, \tilde{\tau})$ . We have the following correspondences in the same manner:

$$\begin{cases} (\rho, w) & \leftrightarrow & (\tilde{\tau} \nu, \tilde{\tau}) \\ (z, q^2) & \leftrightarrow & (\nu, \tau) \\ (qz, q^2) & \leftrightarrow & (\nu + \frac{\tau}{2}, \tau) \\ (z^{-1/2}, q^2) & \leftrightarrow & (-\frac{\nu}{2}, \tau) \end{cases} \quad (\text{A.2})$$

The functions  $\psi$ ,  $\psi^T$  and  $\psi^N$  defined in the text are also the same as those in GSW, and are rewritten as follows in terms of the Jacobi theta functions:

$$\begin{cases} \psi(\rho, w) = -2\pi i e^{\pi i(\tilde{\tau}\nu)^2/\tilde{\tau}} \frac{\vartheta_1(\tilde{\tau}\nu|\tilde{\tau})}{\vartheta_1'(0|\tilde{\tau})} = \frac{2\pi i}{\tau} \frac{\vartheta_1(\nu|\tau)}{\vartheta_1'(0|\tau)}, \\ \psi^T(\rho, w) = 2\pi e^{\pi i(\tilde{\tau}\nu)^2/\tilde{\tau}} \frac{\vartheta_2(\tilde{\tau}\nu|\tilde{\tau})}{\vartheta_1'(0|\tilde{\tau})} = \frac{2\pi}{\tau} e^{\pi i(\nu+\tau/4)} \frac{\vartheta_1(\nu+\frac{\tau}{2}|\tau)}{\vartheta_1'(0|\tau)}, \\ \psi^N(\rho, w) = -2\pi i e^{\pi i(\tilde{\tau}\nu)^2/\tilde{\tau}} \frac{\vartheta_1(\tilde{\tau}\nu|\tilde{\tau}+\frac{1}{2})}{\vartheta_1'(0|\tilde{\tau}+\frac{1}{2})} = -\frac{4\pi i}{\tau} \frac{\vartheta_1(-\frac{\nu}{2}|\frac{\tau}{4}+\frac{1}{2})}{\vartheta_1'(0|\frac{\tau}{4}+\frac{1}{2})}, \end{cases} \quad (\text{A}\cdot 3)$$

where the second equalities follow from the modular transformation properties of the theta functions. Now in view of the correspondences in Eq. (A·2), the comparison of the first and second expressions of  $\psi(\rho, w)$  immediately leads to the relation

$$\psi(\rho, w) = -\frac{1}{\tau} e^{-\pi i\nu^2/\tau} \psi(z, q^2). \quad (\text{A}\cdot 4)$$

Comparison of the second expression of  $\psi^T(\rho, w)$  with the first one of  $\psi(\rho, w)$  gives

$$\psi^T(\rho, w) = \frac{i}{\tau} e^{\pi i(\nu+\tau/4)} e^{-\pi i(\nu+\tau/2)^2/\tau} \psi(qz, q^2) = \frac{i}{\tau} e^{-\pi i\nu^2/\tau} \psi(qz, q^2). \quad (\text{A}\cdot 5)$$

Further, comparing the first and second expressions of  $\psi^N(\rho, w)$ , we obtain

$$\psi^N(\rho, w) = \frac{2}{\tau} e^{\frac{-\pi i(-\nu/2)^2}{\tau/4}} \psi^N(z^{-1/2}, q^{1/2}) = \frac{2}{\tau} e^{-\pi i\nu^2/\tau} \psi^N(z^{-1/2}, q^{1/2}). \quad (\text{A}\cdot 6)$$

Moreover, using  $\vartheta_1(-\nu|\tau) = -\vartheta_1(\nu|\tau)$  and  $e^{\pi i(\nu+\tau)^2/\tau} \vartheta_1(\nu+\tau|\tau) = -e^{\pi i\nu^2/\tau} \vartheta_1(\nu|\tau)$ , we immediately find

$$\begin{cases} \psi(z^{-1}, q^2) = -\psi(z, q^2) \\ \psi(q^2 z, q^2) = -\psi(z, q^2) \end{cases}. \quad (\text{A}\cdot 7)$$

## References

- [1] T. Kugo and T. Takahashi, Prog. Theor. Phys. **99** (1998), 649.
- [2] T. Asakawa, T. Kugo and T. Takahashi, Prog. Theor. Phys. **100** (1998), 831.
- [3] A. LeClair, M. E. Peskin and C. R. Preitschopf, Nucl. Phys. **B317** (1989), 411.
- [4] L. Alvarez-Gaumé, C. Gomez, G. Moore and C. Vafa, Nucl. Phys. **B303** (1988), 411.
- [5] S. B. Giddings and E. Martinec, Nucl. Phys. **B278** (1986), 91.
- [6] T. Kugo and K. Suehiro, Nucl. Phys. **B337** (1990), 434.
- [7] T. Kugo and B. Zwiebach, Prog. Theor. Phys. **87** (1992), 801.
- [8] A. LeClair, M. E. Peskin and C. R. Preitschopf, Nucl. Phys. **B317** (1989), 464.
- [9] Y. Saitoh and Y. Tanii, Nucl. Phys. **B325** (1989), 161.
- [10] Y. Saitoh and Y. Tanii, Nucl. Phys. **B331** (1990), 744.
- [11] K. Kikkawa and S. Sawada, Nucl. Phys. **B335** (1990), 677.
- [12] M. B. Green, J. H. Schwarz and E. Witten, *Superstring Theory*, (Cambridge Univ. Press, Cambridge, 1987).
- [13] T. Asakawa, T. Kugo and T. Takahashi, Prog. Theor. Phys. **100** (1998), 437.
- [14] M. Kaku and K. Kikkawa, Phys. Rev. **D10** (1974), 1823.
- [15] S. Mandelstam, in *Unified String Theories*, ed. by M. Green and D. Gross (World Scientific, Singapore, 1986), p46.

- [16] D. Z. Freedman, S. B. Giddings, J. A. Shapiro and C. B. Thorn, Nucl. Phys. **B298** (1988), 253.
- [17] E. T. Whittaker and G. N. Watson, *A Course of Modern Analysis*, (Cambridge Univ. Press, London, 1927), Chapters XX and XXI.
- [18] M. R. Douglas and B. Grinstein, Phys. Lett. **183B** (1987), 52.
- [19] S. Weinberg, Phys. Lett. **187B** (1987), 278.
- [20] H. Itoyama and P. Moxhay, Nucl. Phys. **B293** (1987), 685.
- [21] N. Ohta, Phys. Rev. Lett. **59** (1987), 176.
- [22] M. Kaku and K. Kikkawa, Phys. Rev. **D10** (1974), 1110.
- [23] E. D'Hoker and S. B. Giddings, Nucl. Phys. **B291** (1987), 90.
- [24] H. Hata, K. Itoh, T. Kugo, H. Kunitomo and K. Ogawa, Phys. Rev. **D34** (1986), 2360.